Title

The light response of mesophyll conductance is controlled by structure across leaf profiles

Journal

Plant Cell & Environment, 40(5)

ISSN

0140-7791

Authors

Théroux-Rancourt, Guillaume

Gilbert, Matthew E

Publication Date

2017-05-01

DOI

10.1111/pce.12890

Peer reviewed

Title: The light response of mesophyll conductance is controlled by structure across leaf profiles

Guillaume Théroux-Rancourt and Matthew E. Gilbert

Department of Plant Sciences, University of California, Davis, 95616, USA

Correspondence: G. Théroux-Rancourt. E-mail: gtrancourt@ucdavis.edu

SUMMARY STATEMENT

Using theoretical and observed evidence of the response of mesophyll conductance (g_m) to light, it is shown that this response is apparent, where the bulk leaf g_m appears to respond to light while layer-specific g_m values do not. This was successfully represented using a multi-layer leaf model coupled with anatomical observations. This apparent response has implications for how limitation analyses are conducted and illustrates the importance of measuring g_m under saturating light. Mesophyll conductance is an emergent property of the 3D leaf structure and not solely a leaf area based phenomenon.

ABSTRACT

Mesophyll conductance to CO_2 (g_m) may respond to light either through regulated dynamic mechanisms or due to anatomical and structural factors. At low light, some layers of cells in the leaf cross-section approach photocompensation and contribute minimally to bulk leaf photosynthesis and little to whole leaf g_m ($g_{m,leaf}$). Thus, the bulk $g_{m,leaf}$ will appear to respond to light despite being based upon cells having an anatomically fixed mesophyll conductance. Such behavior was observed in species with contrasting leaf structure using the variable J or stable isotope method of measuring $g_{m,leaf}$. A species with bifacial structure, *Arbutus* × 'Marina', and an isobilateral species, *Triticum durum* L., had contrasting responses of $g_{m,leaf}$ upon varying adaxial or abaxial illumination. Anatomical observations, when coupled with the proposed model of $g_{m,leaf}$ to PPFD response, successfully represented the observed gas exchange data. The theoretical and observed evidence that $g_{m,leaf}$ apparently responds to light has large implications for how $g_{m,leaf}$ values are interpreted, particularly limitation analyses, and indicates the importance of measuring g_m under full light saturation. Responses of $g_{m,leaf}$ to the environment should be treated as an emergent property of a distributed 3D structure, and not solely a leaf area based phenomenon.

Key-words: photosynthesis; *Arbutus*; *Triticum*; internal conductance; leaf anatomy

INTRODUCTION

Mesophyll conductance to CO_2 (g_m) is understood to be the result of multiple processes within the leaf. In combination, these factors limit photosynthesis by up to 50%. Major limitations to CO_2 diffusion within the leaf include: diffusion in the air from the stomata to the cells, diffusion in solution in the tortuous cell wall, movement through the plasma membrane or aquaporins, diffusion through the cytosol influenced by carbonic anhydrase, and movement through the chloroplast envelopes. Most of these limitations are constant and anatomically determined (Evans *et al.* 2009, Nobel 1999, Terashima *et al.* 2011) and potentially genetically determined (Barbour *et al.* 2016, Jahan *et al.* 2014). However, the hypothesized role of aquaporins (Flexas *et al.* 2006, Perez-Martin *et al.* 2014) and carbonic anhydrase (Ho *et* al. 2016, Tholen & Zhu 2011) may allow the leaf to dynamically control g_m in response to the environment.

A third effect that has not been routinely incorporated into the concepts of g_m response to the environment is the three-dimensional nature of CO_2 diffusion in the leaf (Parkhurst 1986, 1994). In particular, the leaf vertical profile has varying photosynthetic capacity and cellular structure (Evans 2009, Evans and Vogelmann 2003, Ho *et al.* 2016, Verboven *et al.* 2015). Heterogeneities in the intra-leaf light absorption profiles and cell structure have previously allowed researchers to explain the difference between the light responses of leaves illuminated on the adaxial or abaxial side (Oya and Laisk 1976, Terashima 1986, Terashima *et al*. 1986). Similarly, irradiance of different quality, e.g. wavelength, diffuse or direct illumination, penetrates to alternative depths in the leaf (Brodersen and Vogelmann 2010, Evans and Vogelmann 2003, Terashima *et al*. 2009). Also, the ability of chloroplasts to move would lead to changes in the diffusion pathway (Gorton *et al*. 2003) as the surface of chloroplast exposed to the intercellular airspace would change (Ho *et al*. 2016, Tholen *et al*. 2008). Although little change

in leaf g_m has been observed in response to chloroplast movement (Gorton *et al*. 2003, Loreto *et al*. 2009), it is conceivable that changing between diffuse and direct light, or high versus low intensities would lead to dynamic variation in the physical basis for CO_2 diffusion at a local or chloroplast level. Other factors may allow a leaf to display dynamics in g_m, analogous to gating of water transport in aquaporins with light (Prado *et al*. 2013) and changing proportions of photorespiration and respiration in response to C_i as light decreases (Tholen & Zhu 2011). Alternatively, Evans (2009) suggests that varying photosynthetic contributions of cells with different characteristics could lead to apparent changes in g_m.

The response of g_m to light has not been extensively reported to date. With a few studies reporting that g_m remains constant over a range of photosynthetic photon flux density (PPFD) and others showing a slight response. A response was observed from CO_2 response curves measured at three PPFD, where g_m was higher at 1000 than at 250 μmol m^{-2} s^{-1} PPFD (Flexas *et al.* 2007). No response of g_m to PPFD was found using stable isotope methods under 2% [O_2] (Tazoe *et al.* 2009). Neither study reports g_m for low PPFD's (<200 μmol m^{-2} s^{-1}). Yin *et al*. (2009), measuring below 200 μmol m^{-2} s^{-1}, observed a g_m response to PPFD in wheat and account for it by fitting a phenomenological model similar to Leuning's stomatal model (Leuning 1995) where g_m is variable. Thus, it appears that there is a need to investigate the nature of g_m response to light.

The following hypothesis is suggested: leaf g_m responds to PPFD due to changing patterns of light penetration within the leaf leading to different contributions of each layer to bulk leaf g_m ($g_{m,leaf}$). The hypothesis is further developed in the *Theory* section and tested using the modified variable J method, while stable isotope based $g_{m,leaf}$ values were used as confirmation of $g_{m,leaf}$ response to PPFD. Two species were chosen with bifacial or isobilateral

leaf anatomy to provide contrasting profiles of photosynthesis in leaves. As a confirmation of the proposed model, anatomical observations were used to constrain the model, and determine if the observed gas exchange patterns could be replicated by the model. The alternative hypotheses are that either there is no response of $g_{m,leaf}$ to PPFD, or that if a anatomically determined multi-layer leaf photosynthesis model is unable to represent the observed responses, then a dynamic, regulated mechanism of $g_{m,leaf}$ response to light is required.

THEORY

A leaf can be seen as a stack of layers representing the palisade and spongy mesophyll, or a profile (e.g. Parkhurst 1986). Layers can have very different photosynthetic properties and each layer is influenced by the processes occurring in the adjacent layers, for example light absorption, which will influence the CO_2 drawdown resulting from photosynthesis.

The goal of the modeling here was to reconstruct the measured net photosynthesis of a leaf ($A_{n,leaf}$), PPFD absorbed by PSII ($I_{2,j}$) at each layer (j) and the mesophyll conductance ($g_{m,leaf}$) to PPFD relationship from modelled leaf layer values ($A_{n,j}$ and $g_{m,j}$; Fig. 1; see Table 1 for definition of model variables). Applied to the extreme – a leaf with uniform cell characteristics across layers and a constant layer based $g_{m,j}$ – the model would form a null hypothesis (termed null model here) to which leaves with varying layer characteristics could be compared (i.e. the model leaf presented in Fig. 1). The general model would demonstrate if $g_{m,leaf}$ changes with PPFD, based upon variation in the photosynthesis of different layers in the leaf, independent of regulated changes in the diffusion CO_2 pathway. Specifically, if layer-$g_{m,j}$ is constant based upon anatomy, but each layer varies in contribution to total leaf $A_{n,leaf}$, then how does bulk leaf $g_{m,leaf}$ respond to PPFD?

105 The PPFD reaching each layer ($PPFD_j$) is:

106 $$PPFD_j = PPFD_{j-1} - PPFD_{abs,j-1} \quad \text{(eqn. 1)}$$

107 where $PPFD_{abs,j-1}$ is the PPFD absorbed by the layer before, and calculated as:

108 $$PPFD_{abs,j-1} = PPFD_{j-1}\ \alpha_{j-1} \quad \text{(eqn. 2)}$$

109 where α_{j-1} is the absorptance of the previous layer. The effective PPFD for calculating electron
110 transport rates ($I_{2,j}$) is:

111 $$I_{2,j} = PPFD_j\ \alpha_j\ (1\text{-}f_j)\ \beta_j \quad \text{(eqn. 3)}$$

112 where f_j is ~0.15, a spectral quality correction for the relative inefficiency of white light relative
113 to red photons (Evans 1987) and the β_j is typically 0.5, the partitioning between PSII and I (von
114 Caemmerer 2000). The electron transport rate for a layer of the leaf (J_j) is then modelled using
115 the light-response curve equation from Ögren and Evans (1993):

116 $$J_j = \frac{I_{2,j}+J_{max,j}-\sqrt{(I_{2,j}+J_{max,j})^2-4\theta_j I_{2,j} J_{max,j}}}{2\theta_j} \quad \text{(eqn. 4)}$$

117 where $J_{max,j}$ is the maximal electron transport rate of the j'th layer and θ_j is the curvature factor.

118 A constant intercellular airspace CO_2 concentration (C_i) is assumed across the leaf as the
119 intercellular airspace contribution to $g_{m,leaf}$ is low for many species and leaf anatomies (Aalto &
120 Juurola 2002, Piel *et al.* 2002). Although this has been debated (Parkhurst 1994), this assumption
121 has been widely used in profile based modelling and helps to simplify the model without
122 requiring multiple nested simulations to model the layer photosynthetic rates, and recent finite
123 element 3D modelling has shown a mostly constant [CO_2] within the leaf intercellular airspace

(Ho *et al.* 2016). However, the chloroplastic CO_2 concentration ($C_{c,j}$) for each layer of the leaf has to be found using an numerical solution to obtain the gradient for CO_2 diffusion necessary to compute $A_{n,j}$. This is done by minimizing the difference between eqn. 5 and 6 for each layer of the leaf:

$$A_{n,j} = g_{m,j}(C_i - C_{c,j}) \quad \text{(eqn. 5)}$$

and

$$A_{n,j} = (1 - \Gamma^*_j/C_{c,j}) \times \min(V_{c,Rubisco,j}, V_{c,RuBP,j}) - R_{d,j} \quad \text{(eqn. 6)}$$

where:

$$V_{c,Rubisco,j} = C_{c,j}V_{c,max,j}/(C_{c,j} + K_{c,j}(1 + O/K_{o,j})) \quad \text{(eqn. 7)}$$

$$V_{c,RuBP,j} = J_j/(4 + 8\Gamma^*_j/C_{c,j}) \quad \text{(eqn. 8)}$$

and $R_{d,j}$ is the mitochondrial respiration in the light ($\sum_{j=1}^{l} R_{d,j} = R_{d,leaf}$), Γ^*_j is the photosynthetic compensation point in the absence of respiration (same for each layer), $V_{c,Rubisco,j}$ the carboxylation rate under Rubisco-limited conditions, and $V_{c,RuBP,j}$ the carboxylation rate under RuBP-limited conditions. The numerical solution is found for each layer j. In eqn. 5, $g_{m,j}$ is a fixed value specific for each layer j.

The leaf mesophyll conductance can then be calculated based upon a constant $g_{m,j}$ at each layer *and* the weighted contribution of each layer to leaf A_n. This principle can be illustrated by the situation where, as a layer of the leaf tends towards zero net photosynthesis, then the layer contributes a decreasing signal to the measured g_m of the whole leaf. An assimilation-weighted

143 $g_{m,leaf}$ for l layers of the leaf can be computed as per Lloyd *et al*. (1992); see the Appendix of this
144 paper for an alternative derivation of this equation:

145 $$g_{m,leaf} = \frac{A_{n,leaf}}{C_i - \frac{\sum_{j=1}^{l} A_{n,j} C_{c,j}}{A_{n,leaf}}}. \quad \text{(eqn. 9)}$$

146 A useful aspect of the model is that it can be used to simulate the g_m light response of a
147 leaf regardless of the direction of illumination. This modelling approach is used for a leaf with
148 three layers (Fig. 1), for instance two palisade and one spongy mesophyll layers (increasing the
149 number of layers produces a similar response; data not shown). The theoretical leaf presented in
150 Figure 1 was parameterized assuming all layers had the same photosynthetic parameters, termed
151 the null model, i.e. $g_{m,j}$ was equal for each layer and structurally fixed (parameters for the null
152 model are given in the Figure 1 legend). That is, layer based values of $g_{m,j}$ did not vary in the null
153 model, but the contribution of each layer to the whole leaf $g_{m,leaf}$ signal did vary based upon layer
154 specific photosynthetic rates. At high PPFD all layers contributed a similar photosynthesis rate,
155 and thus $g_{m,leaf}$ was roughly the additive values of $g_{m,j}$ (Fig. 1; eqn. 9). Under the lowest PPFD the
156 adaxial layer contributed a higher photosynthesis signal, resulting in that layer contributing the
157 most to $g_{m,leaf}$ while the abaxial layer respired resulting in a *negative* contribution to $g_{m,leaf}$ and a
158 low total $g_{m,leaf}$ value. When the leaf respires, i.e. $A_{n,leaf}$ is negative, then the $g_{m,leaf}$ must increase
159 back to the maximum value as the flux *and* gradient would be inverted (these respiratory
160 responses are at the very left most side of the $g_{m,leaf}$ PPFD response in Fig. 1).

161 However, a caveat of eqn. 9 is that when $A_{n,leaf}$ equals zero then the denominator, the
162 gradient (C_i-C_c), is zero, which makes the estimation of $g_{m,leaf}$ undefined. This is an unavoidable
163 and inherent issue in the common conception of g_m in the form of:

$$g_m = A_n / (C_i - C_c) \quad \text{(eqn. 10)}$$

when C_c equals C_i (see also eqn. 11). Considering this, estimating $g_{m,leaf}$ under low light conditions leading $A_{n,leaf}$ to equal zero is unreliable. This is reached under very low light intensities, below 50 μmol m^{-2} s^{-1} PPFD in our null model of a leaf (Fig. 1). Nonetheless, in a real leaf, this mathematical issue is simply not present and C_i must equal C_c at least twice a day. In that case, g_m as a physical resistance still exists, but would be unmeasurable.

TABLE 1 AND FIGURE 1 COULD BE PLACED HERE.

Thus, it is clear from a theoretical standpoint that $g_{m,leaf}$ must appear to respond to light in a structural manner, consistent with pools of cells contributing to photosynthesis differentially under varying light. Evans (2009) predicted $g_{m,leaf}$ to respond to PPFD in this manner, while Parkhurst (1994) and Lloyd *et al*. (1992) suggested that differing photosynthetic contributions of cells would lead to apparent changes in $g_{m,leaf}$. The rest of this paper is directed to answering:

1) Is such behavior observed in leaves?
2) Are the observed light responses of $g_{m,leaf}$ consistent with constant anatomical characteristics and varying structural (layer) contributions to photosynthesis, or are dynamic, regulated processes necessary to explain the observed light responses?
3) What broader implications does this model of the $g_{m,leaf}$ response to PPFD have for contrasting leaf anatomies, and for the measurement of g_m?

MATERIALS AND METHODS

Species used and plant growth conditions

Arbutus × 'Marina' (*Arbutus unedo* L. × *A. andrachne* L.) year-old saplings were used to represent a leaf with bifacial anatomy and high leaf mass area (LMA: 97.36 g m^{-2}). *Triticum durum* L. cv. Kronos two-month-old seedlings were used to represent a leaf with high photosynthetic capacity and approximately isobilateral anatomy (LMA: 12.34 g m^{-2}).

Arbutus plants were grown outdoors during the fall at the UC Davis Arboretum Nursery in 4 L pots and were transferred to an environmentally-controlled greenhouse for approximately two weeks to acclimate. Temperature was 25/18°C (day/night) and maximal PPFD from sunlight was ~800 µmol m^{-2} s^{-1}. *Triticum* seeds were sown in 4 L pots filled with a coarse substrate (1/3 sand, 1/3 peat, 1/3 redwood compost) in the same greenhouse. Both species were fertigated daily when irrigated.

The flag leaves of *Triticum* were measured; these leaves are positioned at a high angle with illumination occurring from either side, or may even 'flip' presenting the abaxial surface upwards. For *Arbutus*, a fully expanded leaf, with a plastochron index of five to seven, were measured.

Gas exchange: variable J method

Plants were transferred to the lab into a custom-made cabinet (~1.2 m^3), allowing for the control of temperature (maintained at 25±1°C), vapor pressure deficit (VPD; 1.5±0.2 kPa), and PPFD (set at 800 µmol m^{-2} s^{-1} at the top of the plant), and air mixing. A custom gas exchange chamber was used to maximize resolution under low photosynthesis. Leaf gas exchange was measured inside the growth cabinet using a LI-6400XT with a 2x3cm clear top PAM−2000 adaptor chamber (LI-COR Biosciences, Lincoln, NE, USA) and equipped with a PAM−2000 chlorophyll fluorometer (Heinz Walz GmbH, Effeltrich, Germany). PPFD was provided to the leaf by a

white light (LI-COR6400-18A) providing equal quantities of red, blue and green PPFD, and was placed ~2 cm above the leaf surface, with the angle adjusted to avoid the PAM-2000 probe shading the leaf, whilst still illuminating the leaf homogeneously, similar to Bellasio and Griffiths (2014). The chamber was covered with black cloth to shade the leaf from external light. The leaf was allowed to stabilize with the adaxial side being illuminated at leaf chamber CO_2 mole fraction (C_a) of 380 µmol mol^{-1}, PPFD of 1000 µmol m^{-2} s^{-1}, VPD of 1.5±0.1 kPa, flow of 500 µmol s^{-1}, and leaf temperature of 25±0.2°C. Gas exchange was recorded simultaneously with steady state chlorophyll fluorescence under light (F_s) and maximum fluorescence under saturating light (F_m'; ~15000 µmol m^{-2} s^{-1}), used to compute the photochemical efficiency of PSII ($\Phi_{PSII} = (F_m' - F_s) / F_m'$).

Following the measurement under ambient C_a, [CO_2] was increased to lower the photorespiratory bias on g_m estimates when evaluated at low C_i (Tholen & Zhu 2011). A normalized C_i of 280 µmol mol^{-1} was used, which is the minimal C_i at which g_m plateaus; see Théroux-Rancourt *et al*. (2014). A light response curve using adaxial illumination was measured at normalized C_i at PPFD of 950, 500, 350, 230, 140, 85, and 45 µmol m^{-2} s^{-1}. After the last point, the leaf was inverted and equilibrated at 800 µmol m^{-2} s^{-1} PPFD for at least one hour. The leaf was then equilibrated to 950 µmol m^{-2} s^{-1} PPFD before measuring the same light response as above. The lights were then turned off and the plant was shaded with a black cloth, and dark respiration (R_n) was measured after ~20 min. The order in which the sides of the leaves were measured did not affect the light responses (data not shown), and so the adaxial side was chosen as the first side measured.

Mesophyll conductance to CO_2 was estimated using the variable *J* method (Harley *et al.* 1992):

$$g_{\mathrm{m,leaf}} = \frac{A_{\mathrm{n,leaf}}}{C_{\mathrm{i}} - \frac{\Gamma^{*}\,(J_{\mathrm{f}} + 8(A_{\mathrm{n,leaf}} + R_{\mathrm{d,leaf}}))}{J_{\mathrm{f}} - 4\left(A_{\mathrm{n,leaf}} + R_{\mathrm{d,leaf}}\right)}} \qquad \text{(eqn. 11)}$$

where J_f is the photochemical electron transport rate estimated from chlorophyll fluorescence, and Γ* is assumed to be 37.4 μmol mol^{-1} (Bernacchi *et al*. 2002). The use of a normalized and constant C_i for the estimation of g_m limits the potential bias caused by an inaccurate Γ*, which means that the observed response is less sensitive to this issue, as seen in the initial variable *J* method paper (Harley *et al*. 1992) and in one of our previous reports (Théroux-Rancourt *et al*. 2014). Dark respiration was used as a rapid proxy for $R_{d,leaf}$, considered to be half of R_n (Niinemets *et al.* 2009, Théroux-Rancourt *et al.* 2014). The electron transport rate estimated from chlorophyll fluorescence was calibrated according to the following linear relationship (Hassiotou *et al.* 2009):

$$J_f = [\ (\Phi_{PSII}\ s) + c\ ]\ \mathrm{PPFD} \qquad \text{(eqn. 12)}$$

where *s* represents the ratio of Φ_{CO2} (the gas exchange-based photochemical quantum yield) to Φ_{PSII}, and *c* represents the intercept of the relationship between Φ_{PSII} and Φ_{CO2}. Calibration was performed under ambient, 21% O_2 conditions following the method described in Théroux-Rancourt *et al*. (2014). Using detailed A_n-C_i curve analysis combined with chlorophyll fluorescence, *s* was fit using the RuBP-limited version of eqn. 3 of Éthier *et al*. (2006). This method hence solves *s* (and so J_f) and $g_{m,leaf}$ simultaneously using the measured A_n-C_i, Φ_{PSII}, and R_d. The *s* values estimated were between 0.319 and 0.42 for *Arbutus* and between 0.39 and 0.43 for *Triticum*, and *c* values were between 1×10^{-4} and 0 for *Arbutus* and between 0.01 and 0 for *Triticum*.

Gas exchange: stable isotope method

On a separate set of plants from those above, light response curves were performed as above, but the air exiting the LI6400XT cuvette was collected and analyzed for stable isotope composition. A three-way valve was added to the chamber exhaust tube, the third port connected to a ~6 m sampling tube (> 50 cm^3). After measuring $g_{m,leaf}$ as above, but under a flow of 200 µmol s^{-1} to maximize CO_2 drawdown within the cuvette and at PPFD of 950, 700, 450, 350, 230, 120, 80, or 45 µmol m^{-2} s^{-1}, the valve was opened toward the sampling tube and air was allowed to flow for ~5 min, allowing > 20 times air change within the tube. To sample air, the valve was returned to its original direction along the cuvette exhaust route, and 20 cm^3 air was slowly sucked from the tube into a gas-tight glass syringe through a brass luer-lock fitting. The syringe's valve was closed, a needle connected, and the needle was flushed with some of sampled air before injecting 12 ml of air into a vial (10 ml Exetainer, Labco, UK). Air was sampled at different PPFD for *Triticum* (950, 450, 230, and 80 µmol m^{-2} s^{-1}) and *Arbutus* (950, 700, 350, and 120 µmol m^{-2} s^{-1}) as the latter closed stomata rapidly at low PPFD and could not be left for over 10 min below 100 µmol m^{-2} s^{-1} PPFD. Air was then sampled from an empty cuvette to measure the isotopic signature of the incoming air at the same chamber [CO_2] (C_s) as the samples measured above ([CO_2] varied due to normalizing C_i) in order to get the reference carbon isotopic composition of the tank CO_2 (~ -36‰).

Carbon isotopic composition ($\delta^{13}C$) of the air samples was measured within one week of sampling at the UC Davis Stable Isotope Facility using a ThermoScientific PreCon-GasBench system interfaced to a ThermoScientific Delta V Plus isotope ratio mass spectrometer (ThermoScientific, Bremen, Germany). CO_2 was sampled by a six-port rotary valve (Valco, Houston, TX) with an 100µL loop programmed to switch at the maximum CO_2 concentration in

the helium carrier gas. The CO_2 was then separated from N_2O and other residual gases by a Poroplot Q GC column (25m x 0.32mm ID, 45°C, 2.5 mL/min). A pure reference gas (CO_2) was used to calculate provisional $\delta^{13}C$ values. Final $\delta^{13}C$ values were obtained by correction to $\delta^{13}C$ values for laboratory standards (calibrated directly against NIST 8545).

Mesophyll conductance was estimated from photosynthetic parameters and the carbon isotopic discrimination against $^{13}CO_2$ ($\Delta^{13}C$), accounting for the ternary effect (Farquhar & Cernusak 2012) using the equations of Evans and von Caemmerer (2013). $\Delta^{13}C$ was computed as (Evans *et al.* 1986):

$$\Delta = \frac{1000\xi\left(\delta^{13}C_{sam} - \delta^{13}C_{ref}\right)}{1000 + \delta^{13}C_{sam} - \xi\left(\delta^{13}C_{sam} - \delta^{13}C_{ref}\right)} \quad \text{(eqn. 13)}$$

where $\delta^{13}C_{sam}$ and $\delta^{13}C_{ref}$ are the isotopic compositions of the LI6400XT cuvette air with and without a leaf, and $\xi = C_a / (C_a - C_s)$. The value of ξ ranged on average from 8 under 950 µmol m^{-2} s^{-1} PPFD to 50 under 100 µmol m^{-2} s^{-1} PPFD.

Microscopy

Leaves were prepared for microscopy using methods from Bozzola and Russell (1992), and Russin and Trivett (2001). Leaves were fixed in Karnovsky's fixative. Tissues were rinsed with 0.1M PO_4 buffer and post-fixed for 2 h in 1% buffered osmium tetroxide. Leaves were dehydrated with ascending concentrations of ethyl alcohol with three changes at 100%, transitioned 1:1 with propylene oxide, and dehydrated using two changes of pure propylene oxide. Infiltration began using Epon/Spurr's resin in three ascending concentrations with propylene oxide. Finally, three changes of resin with microwave assistance were done before

overnight polymerization in capsules. For light microscopy, semi-thin sections were cut using a Leica Ultracut UCT ultramicrotome and were stained with 2% Methylene Blue/Azure II before being observed at 40× magnification with a Axio Imager A2 microscope (Zeiss, Oberkochen, Germany). For transmission electron microscopy, ultrathin sections were cut using a Diatome diamond knife and picked up on 150 mesh copper grids. The sections were stained with uranyl acetate and lead citrate before viewing with a Phillips CM120 Biotwin (FEI, Hillsboro, OR) and equipped with a Gatan MegaScan 794/20 camera.

For each species, two different leaves were analyzed, with two to three cross sections per leaf, a total of five cross sections per species. Structural traits were analysed using the ImageJ software (Schneider *et al.* 2012). Leaf mesophyll thickness (t) was the average distance between the ad- and abaxial epidermis, and divided to create three artificial layers of equal thickness parallel to the epidermises. For the whole leaf and within each layer, the total area of mesophyll and intercellular airspace (IAS) were measured to estimate the leaf mesophyll porosity: f_{IAS} = area IAS (µm^2) / mesophyll area (µm^2). The length of mesophyll cell wall exposed to the IAS (L_m; µm) was measured in order to compute the surface area of mesophyll exposed to the IAS per leaf area (S_m) as:

$$S_m = \frac{L_m}{W} \times F \qquad \text{(eqn. 14)}$$

where W is the width of the section and F is the curvature correction factor to convert measured length into surfaces. This correction factor was computed following Thain (1983) by measuring, for each layer, the major and minor axes of at least ten cells for two different leaves (F values are shown in Table 2). The whole leaf S_m was computed from the whole leaf average F.

For electron micrographs, the thickness of the cell wall (T_{cw}) and cytosol (T_{cyt}) was measured (> five different cells). The cell wall length exposed to the IAS of individual cells was measured (L_m), the length of chloroplast exposed to the IAS (L_c; μm), and the surface area of chloroplasts exposed to the IAS per leaf area (S_c) equaled:

$$S_c = S_m \times \frac{L_c}{L_m}. \quad \text{(eqn. 15)}$$

S_c was computed for each layer, and the whole leaf S_c was computed from the whole leaf S_m multiplied by the whole leaf average chloroplast coverage of mesophyll cells.

The liquid phase resistance (r'_{liq}) to CO_2 was estimated as the sum of all the liquid phase components in the diffusion path from the cell wall to the stroma using the equations of Evans *et al*. (2009) adjusting anatomy specific lengths. Liquid phase resistance on a chloroplast surface area basis was converted to a leaf area basis to provide an anatomical estimate of g_m using:

$$g_m = \left(1/r'_{liq}\right) S_c. \quad \text{(eqn. 16)}$$

Simulations

The model described in the *Theory* section was used to simulate the sensitivity of $g_{m,leaf}$ to PPFD responses for a two-layer leaf, to vary parameters singly, or used to fit a three-layer model to the mean observed data for the two species. To constrain fitting, the minimum sum of squares was found using the L-BFGS-R constrained optimization algorithm with the *optim* function of R (version 3.3.1). Boundary conditions were set to limit the different parameters within a relevant range. This consisted of limiting the layer-maximum value to the whole leaf maximum or anatomical data ($J_{max,j}$: the whole leaf value fitted from gas exchange and chlorophyll

fluorescence; $g_{m,j}$: maximum layer-specific anatomical value; α_j: the maximum predicted layer-specific α + 10%, generated according to the relative S_c profile constrained to yield a total leaf absorption of 0.85 (layer-specific α values represent the fraction of light absorbed within that layer – generated using equations 1 and 2 – and not the fraction of the total incoming light)). For $R_{d,j}$, a high upper boundary was set to (5 µmol m^{-2} s^{-1}), and θ_j was constrained between 0.0001 and 0.9999.

The relative anatomically based relationship between each layer was also included in the fitting procedure so that the resulting parameters would follow a profile similar to the observed anatomy. Specifically, fitting SSE was penalized if $J_{max,i}$ and $R_{d,i}$ did not follow the relative profile in S_c, while $g_{m,i}$ followed the profile in g_m estimated from anatomy (Table 2). This allowed for different absorption profiles depending on the illuminated surface, while providing a unique value for each layer. This value corresponded to the absorbed fraction of incoming light at layer *j*, thus taking into account the absorbed fraction at layer *j-1*. Total leaf absorption was constrained to 0.85, a value commonly used in the literature (e.g. Evans 2009).

The sum of squares to be minimized was the sum of nine constraints, i.e. the squared differences between: i) $A_{n,leaf}$ observed and predicted by the model for ad- and abaxial illumination, ii) $g_{m,leaf}$ observed and predicted for ad- and abaxial illumination, iii) the $C_{c,j}$ values input and those predicted by using the result of eqn. 6 and calculating $C_{c,j}$ from rearranging eqn. 5, iv) predicted whole leaf absorptance and a default value of 0.85, v) the observed and predicted initial slope of the $A_{n,leaf}$ to PPFD response for ad- and abaxial illumination, and vi)-ix) the sum of the squared difference between the reference relative profile and the fitted relative profile for $J_{max,j}$, $g_{m,j}$, $R_{d,j}$, and α_j. Each constraint was weighted so that the resultant sum of squares for each was within one order of magnitude of the others.

The optimization was ran on over 500 sets of starting values that followed the relative profiles in S_c ($J_{max,j}$, $g_{m,j}$, $R_{d,j}$) or values from the literature (α_j), and starting values for θ_j were selected randomly between 0.001 and 0.999. Solutions within 10% of the SSE of the best fit were selected. For α_j, we validated the fit gradient based upon measurements of S_c profiles by contrasting it to the published absorption profiles of a bifacial leaf (spinach; Evans and Vogelmann 2003) and an isobilateral leaf (eucalyptus; Evans and Vogelmann 2006) to represent *Arbutus* and *Triticum*, respectively.

RESULTS

Response of net photosynthesis and mesophyll conductance to PPFD

The bulk net photosynthesis of *Triticum* and *Arbutus* were typical of reported responses to irradiance from adaxial illumination (Fig. 2). However, leaf mesophyll conductance varied approximately proportionally with net photosynthesis at lower PPFD (Fig. 2). A switch from adaxial to abaxial illumination had similar effects on the $A_{n,leaf}$ and $g_{m,leaf}$ of *Arbutus* with a ~40% decrease. In contrast, the isobilateral leafed species, *Triticum*, had similar photosynthesis regardless of the side of illumination, but a large decrease in $g_{m,leaf}$ upon abaxial illumination. The C_i was kept constant at 280 μmol mol^{-1} during the PPFD responses. Thus, the observed responses are not due to an apparent response of g_m to CO_2 concentration.

The stable isotope method of estimating $g_{m,leaf}$ was used to establish whether the variable *J* chlorophyll fluorescence based method could have biases that led to the response of $g_{m,leaf}$ to PPFD. Response curves measured simultaneously using the chlorophyll fluorescence and stable isotope methods showed similar responses of $g_{m,leaf}$ to PPFD (Fig. 3). The estimated values of

383 $g_{m,leaf}$ using both methods were directly proportional to each other, indicating that the curved
384 $g_{m,leaf}$ response to PPFD was not due to a bias by the chlorophyll fluorescence method. However,
385 as is typical in the literature (e.g. Vrábl *et al.* 2009), the two methods had quantitatively different
386 absolute values.

387 FIGURES 2 AND 3 COULD BE PLACED HERE

388

389 ## Anatomical description of leaves and layer specific structural parameters

390 Dividing the leaves into three equal-depth layers led to distinct profiles of anatomy in both
391 bifacial *Arbutus* and isobilateral *Triticum* (Fig. 4; Table 2). For *Arbutus*, this clearly separated a
392 dense palisade layer of one cell of ~80 µm length adjacent to the adaxial epidermis, followed by
393 a loose palisade of two blunt cylindrical cell layers, and four-layers of loosely-packed spheroid
394 to cylindrical cells in the spongy mesophyll adjacent to the abaxial epidermis, where all stomata
395 were located (i.e. a hypostomatous leaf) (see Table 2). *Triticum* showed a more symmetrical
396 profile from adaxial to abaxial epidermis, with a layer of one cylindrical palisade cell of ~50 µm
397 length touching both epidermises, and a spongy-like middle layer composed of spheroid and
398 invaginated cells typical of grasses (e.g. Giuliani *et al*. 2013). The abaxial epidermis was more
399 porous because of the presence of more stomata per section width, hence more substomatal
400 cavities which increase the fraction of intercellular airspace.

401 TABLE 2 AND FIGURE 4 COULD BE PLACED HERE.

402 *Arbutus* leaves were thicker and had higher mesophyll cell wall area (S_m) and chloroplast
403 area (S_c) per unit leaf area than *Triticum* (Table 2), although *Triticum* showed a higher exposed
404 surface on a mesophyll volume basis (0.14 (*Triticum*) vs. 0.10 (*Arbutus*) µm^{-1}; see Nelson *et al.*

2005 about the use of this metric). *Arbutus* had similar values of S_m and S_c in the adaxial and middle layers, and these values decreased in the abaxial layer. *Triticum* had high values on both the ad- and abaxial surfaces and lower values in the center (Table 2). A similar pattern was found in cell wall thickness (T_{cw}), *Arbutus* had an increasing gradient and *Triticum* a low-high-low pattern. Cytoplasm thickness (T_{cyt}) varied less between cell layers, and *Triticum* had a ~three times smaller T_{cyt} than *Arbutus*.

Layer-based modelling of leaf photosynthesis and mesophyll conductance

A three-layer model (*Theory*) was able to represent the observed gas exchange data for either species, including the response of $g_{m,leaf}$ to ad- or abaxial illumination (Fig. 2). In the model, the $g_{m,j}$ values for each layer remained constant, while the weighted values vary resulting in changing $g_{m,leaf}$ (estimated from eqn. 9). The resulting whole leaf values fit the measured $A_{n,leaf}$ values for both species relatively well (Fig. 2). The measured and predicted values for *Arbutus* were similar for the three-layer model, and the range of the best solutions was narrow. The range of the solutions was wider for *Triticum* and there was disagreement between the fitted and measured $g_{m,leaf}$ data in the range of about 125 to 500 µmol m^{-2} s^{-1} PPFD,.

The cause of the varying contribution of each layer to $g_{m,leaf}$ was due to changing layer-specific A_n values (Fig. 5). Only the directly illuminated layers approached saturation, while all other layers had considerably lower photosynthesis, decreasing the $g_{m,j}$ signal from those layers. For this reason, the $g_{m,leaf}$ response was considerable when PPFD was lower than 500 µmol m^{-2} s^{-1}. The low photosynthesis in the adaxial and middle layers in *Arbutus* with abaxial illumination led to the lower $g_{m,leaf}$ than expected from adaxial illumination response (Fig. 2 and 5).

To parameterize the model, the parameters were fit to the gas exchange data, but constrained by the observed relative anatomical profiles for a number of characteristics. Thus, *Triticum* presented an even g_m profile throughout the leaf from the adaxial to the abaxial epidermis (average values of 0.07 mol m^{-2} s^{-1} for each layer; Fig. 6), which followed the relative S_c profile and anatomically based g_m profile (Table 2). *Arbutus* also followed the relative profile in S_c and anatomically based g_m with average $g_{m,j}$ values of 0.06, 0.06, and 0.03 mol m^{-2} s^{-1} from ad- to abaxial epidermis. The fitting of a relative profile was necessary, as the anatomical correlate of J_{max} and R_d, S_c, is not scaled, and the anatomical estimate of g_m is likely to be an overestimate, accounting for only idealized conditions.

$J_{max,j}$ and $R_{d,j}$ were similarly constrained by the S_c relative profile (Fig. 6, Table 2). Layer-specific g_m values presented a very narrow range, as were $R_{d,j}$ values, whereas $J_{max,j}$ had greater variation, but still resulted in a similar whole leaf value (Fig. 2) to layer-specific light response curves (Fig. 5). The leaf based parameter values were additive values for $J_{max,j}$ and $g_{m,j}$ representing a value close to the whole leaf measured (g_m) or estimated value (J_{max}). For the sum of $R_{d,j}$, this was a somewhat high value compared to what was measured (between 0.5 and 1.2 μmol m^{-2} s^{-1}).

The light response curvature (θ_j) exhibited the most variation within each layer as it was not constrained to a specific profile, but the median of each layer was above 0.70 for each species (Fig. 6). Layer specific absorptance (α_j) was relatively constrained within each species, displaying little variation between fits (Fig. 6). In order to compare the fitted data with Evans and Vogelmann's (2003, 2006) data, absorption profiles were produced for ad- and abaxial illumination (Fig. 7). The value for each layer was computed using equations 1 and 2, and the resulting layer-specific PPFD value was divided by sum of the PPFD absorbed. For Evans and

Vogelmann's data, the absorption profile was split into three equal thickness layers for both blue and green light. From these profiles, the median fits for *Triticum* were consistent with the observed data for the isobilateral *Eucalyptus*, regardless of direction of illumination. In contrast, for *Arbutus*, the light absorption profiles predicted from the fit, were only similar to bifacial spinach for abaxial illumination (Fig. 7).

FIGURES 5, 6 AND 7 COULD BE PLACED HERE.

To investigate the impact of each parameter on the $g_{m,leaf}$ to PPFD response, the results of the layer-based model were tested for sensitivity of the $g_{m,leaf}$ to PPFD relationship to parameter values for each layer using a minimal two layer model. At a low PPFD, a 50% decrease in the parameter value of the lower layer, i.e. the layer the furthest away from the light source, resulted in most sensitivity for α_2 (α_j of the lower, second layer), then $R_{d,2}$ and little sensitivity for the θ_2, $J_{max,2}$ or $g_{m,2}$ (Fig. 8). But at high PPFD all parameters had effects on the $g_{m,leaf}$ to PPFD response, in the following order, from the greatest to the smallest effect: $g_{m,2}$, α_2, $J_{max,2}$, θ_2, $R_{d,2}$. As the estimation of $g_{m,leaf}$ is undefined at $A_{n,leaf}$ values close to zero (between -0.1 and 0.1 µmol m^{-2} s^{-1}), these values were removed from Fig. 8. Yet, a high and 'jumpy' sensitivity to parameter values at very low PPFD remains and was due to $g_{m,leaf}$ being affected by CO_2 loss out of the leaf and calculation from low fluxes in eqn. 9 (a low denominator; see the *Theory* section).

FIGURE 8 COULD BE PLACED HERE.

DISCUSSION

Structural variation in photosynthesis across the leaf explains the $g_{m,leaf}$ response to PPFD

Two species of plants with contrasting leaf anatomy both displayed large decreases in the total mesophyll conductance to CO_2 using the modified variable *J* method (Fig. 2) or stable isotopes (Fig. 3). The modelling of layer-based photosynthesis within the leaf could account for the observed responses of $g_{m,leaf}$ to PPFD despite layer-based $g_{m,j}$ being held constant (Fig. 5 and 6).

From the results and theory above, it appears that even if g_m per leaf layer is constant and structurally based then this can result in apparently dynamic responses of $g_{m,leaf}$ to light. Mesophyll conductance response to PPFD has not been investigated in detail in the literature before, to our knowledge, although Evans (2009) suggested the principle upon which the modelling is based. The current observed response of $g_{m,leaf}$ to PPFD is difficult to compare to past reports. Firstly, the most dramatic decrease in $g_{m,leaf}$ occurs at the lowest PPFD's, while past responses were measured at PPFD's of greater than 200 µmol m^{-2} s^{-1} (Flexas *et al.* 2007, Tazoe *et al.* 2009, Yamori *et al.* 2010). Indeed, the null model (Fig. 1) had only a ~30% decrease in $g_{m,leaf}$ at a PPFD of 150 µmol m^{-2} s^{-1}, but rapidly dropped near zero at lower PPFD. Yin *et al.* (2009) did measure below 200 µmol m^{-2} s^{-1}, but did not keep C_i constant. Indeed, if C_i is variable during the measurement of the PPFD response there may be a compensatory effect. That is, at higher C_i's, which occur at low light, $g_{m,leaf}$ may increase due to the positive CO_2 effect at low C_i's (Tholen & Zhu 2011). The results here were partially de-trended of this effect as C_i was kept constant. Previous experiments did not maintain C_i constant when measuring light responses (Flexas *et al.* 2007, Tazoe *et al.* 2009, Yamori *et al.* 2010).

Anatomical profiles predict the observed gas exchange responses

493 The model proposed here was able to accurately represent the observed gas exchange data, when
494 parameterized by the relative profiles of the species anatomical features (S_c and g_m). The
495 observed g_m to PPFD responses are consistent with the observed anatomy. Thus, the modelling
496 results can be used to investigate within-leaf profiles in photosynthetic parameters (J_{max}, g_m, and
497 R_d). Interestingly, the various solutions for *Arbutus* and *Triticum* were in very narrow range of
498 parameters for parameters like $g_{m,j}$, $R_{d,j}$, and α_j, while more variation in absolute values were fit
499 for $J_{max,j}$ and θ_j (Fig. 6). However, *Triticum* exhibited more variation than *Arbutus*, where $g_{m,j}$, θ_j,
500 and $J_{max,j}$ showed a few outlier groups.

501 The only parameter that somewhat diverges from the expected profile is α_j, the layer
502 specific absorptance. For *Triticum*, the light absorption profile was close to what was expected
503 from the isobilateral *Eucalyptus pauciflora* using ^{14}C assimilation profiles (Fig. 7; Evans and
504 Vogelmann 2006). As leaves of *Triticum* can easily move with wind, the absorptance profile may
505 reflect the ability to take full advantage of the light independent of the illuminated surface. For
506 *Arbutus*, the abaxial layer absorbs a higher amount of light which could be explained by the
507 increased scattering due to the more random distribution of the cells in the spongy mesophyll, as
508 shown by Evans and Vogelmann (2003). However, the adaxial and middle layers have lower
509 values than what would be expected from the bifacial spinach of Evans and Vogelmann (2003).
510 Although the α_j values for those two layers could be underestimated compared to Evans and
511 Vogelmann (2003) and to S_c, a proxy for chloroplast volume, the values do follow an anatomical
512 trend as those two layers consist mainly of palisade mesophyll known to channel light to the
513 deeper layers of the leaf (Vogelmann 1993). Nonetheless, the important differences in the fitted
514 light absorption profile for adaxial illumination and the profile for Evans and Vogelmann (2003)
515 data are a result of the simulation procedure, for which the abaxial illumination seemed to weigh

more on the final parameter values than the photosynthesis data measured with adaxial illumination. Hence, the predicted photosynthetic parameter values for each layer, based upon the model, are not necessarily robust even if they are mostly in a range expected based upon anatomy, but do give an indication of the layer based parameters required to result in the observed responses.

Limitations to this analysis

The modelling conducted here does not account for variation in CO_2 diffusion pathways through the mitochondrion due to photorespiration and respiration (Tholen & Zhu 2011). Thus at very low light (< ~25 μmol m^{-2} s^{-1}) or [CO_2], conditions where respiratory CO_2 evolution is high, the current model will over predict values for $g_{m,leaf}$. These light conditions were not investigated in the current work, and thus should not affect the current results, but these effects may be usefully incorporated in future investigations.

The variable *J* method has known sensitivity to calibration conditions (Gilbert *et al.* 2012) and is based upon chlorophyll fluorescence accurately estimating the quantum yield of the leaf profile (Evans 2009). The former issue was dealt with by calibrating the variable *J* method using the modified calibration approach of Théroux-Rancourt *et al.* (2014), moderate to low PPFD's and by reducing noise through the use of a three times larger leaf area than is standard for fluorescence with the LI-6400XT. The potential for a gradient in chlorophyll fluorescence signal from within the leaf does pose a problem for the variable *J* method. The discrepancies between the measured and fitted responses in the 125 to 500 μmol m^{-2} s^{-1} PPFD region can arise from a potential artifact from the chlorophyll fluorescence measurement. As pointed out by

Oguchi *et al*. (2011), chlorophyll fluorescence using a PAM fluorometer (a Walz PAM 101 in their case) leads to the measurement of a weighted signal corresponding to ~200 to 250 µm below the epidermis. Hence, when under PPFD that saturates one layer but not the deeper layers, the resulting signal might potentially be biased towards higher Φ_{PSII} values than the entire leaf, causing measurement errors in the variable *J* method. However, the stable isotope method is robust to this issue, as it does not rely on chlorophyll fluorescence. Stable isotopes confirmed the observed drop in $g_{m,leaf}$ at low PPFD. Given the mathematical proof that $g_{m,leaf}$ should respond to PPFD, it can be expected that regardless of any methodological limitations, that bulk g_m apparently varies with light.

Another limitation of this study could come from chloroplast movement. Mesophyll conductance increases as a consequence of the increase in S_c when chloroplasts move from the profile to the face position, as would happen in a shift from strong white light to blue-filtered light (Tholen *et al*. 2008). As blue light is mainly absorbed close to the illuminated surface, chloroplasts deeper in the leaf would migrate to the cell faces, implying that S_c would dynamically increase in the middle and furthest layer from the light source. Potentially this effect would allow $g_{m,j}$ to increase and slightly increase the apparent $g_{m,leaf}$ signal. It would be interesting to target chloroplast movement as a regulated light response of g_m.

General $g_{m,leaf}$ responses to PPFD for diverse leaves

General predictions can be made on how the $g_{m,leaf}$ of diverse anatomies will respond to light. Leaves that do not saturate photosynthesis are likely to have $g_{m,leaf}$ that responds to PPFD (null model; Fig. 9), because the gradient of $A_{n,j}$ changes with depth and thus affects the $g_{m,leaf}$ measured. However, if the gradient in $g_{m,j}$ matches the gradient in $A_{n,j}$ (null model with $g_{m,j}$

gradient; Fig. 9) or α_j compensates so that $A_{n,j}$ is constant across the leaf (null model with α_j gradient; Fig. 9) then $g_{m,leaf}$ will respond less to PPFD. Leaves that saturate photosynthesis under low light, i.e. with low photosynthetic capacities (low $J_{max,j}$ model; Fig. 9) will have a more even distribution of $A_{n,j}$ through the leaf and thus less $g_{m,leaf}$ response to PPFD. In leaves where multiple photosynthetic parameters vary across the leaf, more diverse responses of $g_{m,leaf}$ to PPFD occur, including steeper positive responses, or even a slight negative responses where $g_{m,leaf}$ decreases at high PPFD. Furthermore, environments with illumination from both sides of the leaf, or with significant diffuse light should lead to a very flat response of $g_{m,leaf}$ to PPFD. Finally, significant gradients in C_i across the leaf intercellular airspace would amplify the observed $g_{m,leaf}$ response to PPFD as both C_i and C_c used in the calculation of $g_{m,leaf}$ would be poorly represented by an average value, a point already raised by Parkhurst (1994).

Hence, maximum $g_{m,leaf}$ can be measured only when all layers are saturated with PPFD, implying that illumination from both sides of the leaf is important for leaves with thick cross-sections or lots of chlorophyll, or for leaves that lack saturation of $A_{n,leaf}$ under full sunlight. But for many leaves, $g_{m,leaf}$ measured at full sunlight will be adequate to approximately match maximum $g_{m,leaf}$.

FIGURE 9 COULD BE PLACED HERE.

Implications for photosynthetic limitation analysis, spectral quality responses, and canopy photosynthesis

In the model presented here, the layer based value of mesophyll conductance, $g_{m,j}$, does not vary, but the leaf value apparently does. Specifically, if $g_{m,j}$ is constant with PPFD, then on a layer basis photosynthesis ($A_{n,j}$) is not limited dynamically by $g_{m,j}$ at different PPFD's. If this effect is

583 generally true, variation in $g_{m,leaf}$ with changing PPFD does not represent a dynamic limitation to
584 photosynthesis. Thus, photosynthetic limitation analyses, e.g. Grassi & Magnani (2005), should
585 avoid making conclusions based upon data sets in which $g_{m,leaf}$ was measured at varying PPFD.
586 Measurements of daily time courses under natural light conditions should be avoided, as the
587 PPFD effect on $g_{m,leaf}$ might add another confounding effect on the g_m response to the
588 environment. Measuring leaves under natural conditions but above a certain PPFD (e.g. Grassi *et*
589 *al.* 2009) may provide a suitable alternative as it is under high PPFD that variations in $g_{m,j}$ and
590 $J_{max,j}$ would lead to least error in the estimates of $g_{m,leaf}$ (Fig. 9), particularly for thin leaves.
591 Limitation analysis seems only appropriate for constant light settings, and most appropriate
592 under high light conditions, especially when comparing leaves of different anatomy (e.g. sun
593 versus shade leaves, developmental stages). Similarly, modelling a variable $g_{m,leaf}$ response to the
594 environment phenomenologically (Yin *et al.* 2009) would result in apparent limitations to
595 photosynthesis under low light conditions, that are actually RuBP-regeneration limitations and
596 not diffusional limitations.

597 The theoretical basis for the $g_{m,leaf}$ to PPFD response suggested here could provide an
598 alternative explanation as to why g_m was previously found to respond to blue light (Loreto *et al.*
599 2009). The reported response of $g_{m,leaf}$ to blue light was rapid and unrelated to chloroplast
600 movement (Loreto *et al.* 2009). A possible explanation for the effect may be that the red and blue
601 light applied differed in depth of penetration at the low PPFD used in former experiment (300
602 µmol m^{-2} s^{-1}). If red and blue light penetrated to different depths, as shown previously (e.g.
603 Brodersen & Vogelmann 2010, Evans and Vogelmann 2006 (see also Fig. 7), Oguchi *et al.* 2011,
604 Vogelmann & Han 2000), then varying $g_{m,j}$ and photosynthetic capacity with depth in the species

used could account for the apparent changes in leaf $g_{m,leaf}$ reported by Loreto *et al*. (2009) for blue light.

An analogous model of layer based photosynthesis, to the one suggested here, could be created for layers of leaves in canopies. If so, the emergent response of canopy g_m to light or other environmental factors would also be apparently responsive if the relative photosynthetic contribution of each layer of leaves varied with the environmental factor. This effect would provide alternative explanations to previously observed data. Possible examples are that bulk canopy g_m varied with ABA application (Schäeufele *et al.* 2011), and could be explained if the photosynthesis varied between leaves (i.e. though an ABA effect), but the $g_{m,leaf}$ remained constant for leaves of varying age. The large apparent variation in canopy g_m estimated from eddy-covariance (Keenan *et al.* 2010) seems likely to be highly dependent upon this effect; where differing contributions of leaf layers to eddy-covariance with changing light and drought are highly likely. In that case, the observed limitation on canopy photosynthesis is likely due to RuBP-regeneration (light), and only apparently due to the calculated decreasing canopy g_m.

Concluding remarks

Fluxes such as net photosynthetic rate are comprised of the additive contributions of all cells in the leaf. As a result, the true net photosynthesis for a leaf can be unambiguously measured. Mesophyll conductance to CO_2 is a conductance, not a flux, having a photosynthetic rate (flux), a potentially variable source (C_i or $C_{i,j}$) and a sink ($C_{c,j}$) that varies cell by cell (e.g. eqn. 9). For instance, leaf C_c does not exist as a discrete value in any leaf, as each layer must have different values for $C_{c,j}$ as pointed out by Parkhurst (1994), but the impact of this on photosynthetic

627 modelling remains to be fully investigated. In general, this means that $g_{m,leaf}$ is an emergent
628 property of many leaf anatomical traits adding up to structure in its true three-dimensional
629 nature. Thus, $g_{m,leaf}$ can appear to respond to environmental variables such as light, despite no
630 structural changes in the basis of CO_2 diffusion in the leaf. To our knowledge, the data presented
631 here are the first non-anatomical evidence that indicate that there are gradients in cellular
632 mesophyll conductance across the leaf profile. While the observed responses of $g_{m,leaf}$ to light are
633 fully consistent with an anatomical, structural or 3D nature of leaf, the results do not preclude a
634 dynamic, regulated response of $g_{m,leaf}$ to PPFD. If the latter responses exist, then the relative
635 weight of the structural and dynamic responses would vary, the former being fixed in time during
636 leaf growth, while the latter, if present, would allow for a shorter timescale control of CO_2
637 diffusion.

638

639 ## CONFLICTS OF INTEREST

640 The authors have no conflicts of interest to declare.

641

642 ## ACKNOWLEDGMENTS

643 We thank Tom Sharkey and two anonymous reviewers for their comments, Pat Kysar for
644 technical assistance with the TEM, Rick Doucett of the UC Davis Stable Isotope Facility, and
645 Taylor Louie of the UC Davis Arboretum Nursery. G.T.-R. was supported by an Esau
646 Postdoctoral Fellowship and a postdoctoral scholarship from the *Fonds de recherche du Québec*
647 *– Nature et technologie,* and M.E.G was supported by USDA NIFA, Hatch project #1001480.

648

REFERENCES

Aalto T. & Juurola E. (2002) A three-dimensional model of CO_2 transport in airspaces and mesophyll cells of a silver birch leaf. *Plant, Cell & Environment*, **25**, 1399-1409.

Barbour M.M., Bachmann S., Bansal U., Bariana H. & Sharp P. (2016) Genetic control of mesophyll conductance in common wheat. *New Phytologist*, **209**, 461-465.

Bellasio C. & Griffiths H. (2014) Acclimation to low light by C4 maize: implications for bundle sheath leakiness. *Plant, Cell & Environment*, **37**, 1046–1058.

Bernacchi C.J., Portis A.R., Nakano H., von Caemmerer S. & Long S.P. (2002) Temperature response of mesophyll conductance. Implications for the determination of Rubisco enzyme kinetics and for limitations to photosynthesis in vivo. *Plant Physiology*, **130**, 1992-1998.

Bozzola J. & Russell L. (1992) *Quantitative electron microscopy*. Jones & Bartlett Learning.

Brodersen C.R. & Vogelmann T.C. (2010) Do changes in light direction affect absorption profiles in leaves? *Functional Plant Biology*, **37**, 403-412.

von Caemmerer S. (2000) *Biochemical models of leaf photosynthesis*. CSIRO Publishing.

Éthier G., Livingston N., Harrison D., Black T. & Moran J. (2006) Low stomatal and internal conductance to CO_2 versus Rubisco deactivation as determinants of the photosynthetic decline of ageing evergreen leaves. *Plant, Cell & Environment*, **29**, 2168-2184.

Evans J.R. (1987) The dependence of quantum yield on wavelength and growth irradiance. *Functional Plant Biology*, **14**, 69-79.

Evans J.R. (2009) Potential errors in electron transport rates calculated from chlorophyll fluorescence as revealed by a multilayer leaf model. *Plant and Cell Physiology*, **50**, 698-706.

672 Evans J.R., Sharkey T., Berry J. & Farquhar G. (1986) Carbon isotope discrimination measured
673 concurrently with gas exchange to investigate CO_2 diffusion in leaves of higher plants.
674 *Functional Plant Biology*, **13**, 281-292.
675 Evans J.R., Caemmerer S., Setchell B.A. & Hudson G.S. (1994) The relationship between CO_2
676 transfer conductance and leaf anatomy in transgenic tobacco with a reduced content of
677 Rubisco. *Functional Plant Biology*, **21**, 475-495.
678 Evans J.R. & Vogelmann T.C. (2003) Profiles of ^{14}C fixation through spinach leaves in relation
679 to light absorption and photosynthetic capacity. *Plant, Cell & Environment*, **26**, 547-560.
680 Evans J.R. & Vogelmann T.C. (2006) Photosynthesis within isobilateral *Eucalyptus pauciflora*
681 leaves. *New Phytologist*, **171**, 771-782.
682 Evans J.R., Kaldenhoff R., Genty B. & Terashima I. (2009) Resistances along the CO_2 diffusion
683 pathway inside leaves. *Journal of Experimental Botany*, **60**, 2235-2248.
684 Evans J.R. & Von Caemmerer S. (2013) Temperature response of carbon isotope discrimination
685 and mesophyll conductance in tobacco. *Plant, Cell & Environment*, **36**, 745-756.
686 Farquhar G.D. & Cernusak L.A. (2012) Ternary effects on the gas exchange of isotopologues of
687 carbon dioxide. *Plant, Cell & Environment*, **35**, 1221-1231.
688 Flexas J., Diaz-Espejo A., Galmes J., Kaldenhoff R., Medrano H. & Ribas-Carbo M. (2007)
689 Rapid variations of mesophyll conductance in response to changes in CO_2 concentration
690 around leaves. *Plant, Cell & Environment*, **30**, 1284-1298.
691 Flexas J., Ribas-Carbo M., Hanson D.T., Bota J., Otto B., Cifre J., McDowell N., Medrano H. &
692 Kaldenhoff R. (2006) Tobacco aquaporin NtAQP1 is involved in mesophyll conductance
693 to CO_2 in vivo. *Plant Journal*, **48**, 427-439.

694 Gilbert M., Pou A., Zwieniecki M. & Holbrook M. (2012) On the measurement of mesophyll
695 conductance to carbon dioxide with the variable *J* method. *Journal of Experimental*
696 *Botany*, **63**, 412-425.
697 Giuliani R., Koteyeva N., Voznesenskaya E., Evans M.A., Cousins A.B. & Edwards G.E. (2013)
698 Coordination of leaf photosynthesis, transpiration, and structural traits in rice and wild
699 relatives (genus *Oryza*). *Plant Physiology*, **162**, 1632-1651.
700 Grassi G. & Magnani F. (2005) Stomatal, mesophyll conductance and biochemical limitations to
701 photosynthesis as affected by drought and leaf ontogeny in ash and oak trees. *Plant, Cell*
702 *& Environment*, **28**, 834-849.
703 Grassi G., Ripullone F., Borghetti M., Raddi S. & Magnani F. (2009) Contribution of diffusional
704 and non-diffusional limitations to midday depression of photosynthesis in *Arbutus unedo*
705 L. *Trees*, **23**, 1149-1161.
706 Gorton H.L., Herbert S.K. & Vogelmann T.C. (2003) Photoacoustic analysis indicates that
707 chloroplast movement does not alter liquid-phase CO_2 diffusion in leaves of *Alocasia*
708 *brisbanensis*. *Plant Physiology*, **132**, 1529-1539.
709 Harley P.C., Loreto F., Di Marco G. & Sharkey T.D. (1992) Theoretical considerations when
710 estimating the mesophyll conductance to CO_2 flux by analysis of the response of
711 photosynthesis to CO_2. *Plant Physiology*, **98**, 1429-1436.
712 Hassiotou F., Ludwig M., Renton M., Veneklaas E.J. & Evans J.R. (2009) Influence of leaf dry
713 mass per area, CO_2, and irradiance on mesophyll conductance in sclerophylls. *Journal of*
714 *Experimental Botany*, **60**, 2303–2314.
715 Ho Q.T., Berghuijs H.N., Watté R., Verboven P., Herremans E., Yin X., Retta M.A., Aernouts
716 B., Saeys W. & Helfen L. (2016) Three-dimensional microscale modelling of CO_2

transport and light propagation in tomato leaves enlightens photosynthesis. *Plant, Cell & Environment*, **39**, 50-61.

Jahan E., Amthor J.S., Farquhar G.D., Trethowan R. & Barbour M.M. (2014) Variation in mesophyll conductance among Australian wheat genotypes. *Functional Plant Biology*, **41**, 568-580.

Keenan T., Sabate S. & Gracia C. (2010) The importance of mesophyll conductance in regulating forest ecosystem productivity during drought periods. *Global Change Biology*, **16**, 1019-1034.

Leuning R. (1995) A critical appraisal of a combined stomatal-photosynthesis model for C3 plants. *Plant, Cell & Environment*, **18**, 339-355.

Lloyd J., Syvertsen J., Kriedemann P. & Farquhar G. (1992) Low conductances for CO_2 diffusion from stomata to the sites of carboxylation in leaves of woody species. *Plant, Cell & Environment*, **15**, 873-899.

Loreto F., Tsonev T. & Centritto M. (2009) The impact of blue light on leaf mesophyll conductance. *Journal of Experimental Botany*, **60**, 2283-2290.

Morris P. & Thain J. (1983) Improved methods for the measurement of total cell surface area in leaf mesophyll tissue. *Journal of Experimental Botany*, **34**, 95-98.

Nelson, E.A., Sage, T.L. & Sage, R.F. (2005) Functional leaf anatomy of plants with crassulacean acid metabolism. *Functional Plant Biology*, **32**, 409-419.

Niinemets U., Wright I.J. & Evans J.R. (2009) Leaf mesophyll diffusion conductance in 35 Australian sclerophylls covering a broad range of foliage structural and physiological variation. *Journal of Experimental Botany*, **60**, 2433-2449.

Nobel P.S. (1999) *Physicochemical and environmental plant physiology*. Academic Press.

740 Ögren E. & Evans J. (1993) Photosynthetic light-response curves. *Planta*, **189**, 182-190.
741 Oguchi R., Douwstra P., Fujita T., Chow W.S. & Terashima I. (2011) Intra-leaf gradients of
742 photoinhibition induced by different color lights: implications for the dual mechanisms of
743 photoinhibition and for the application of conventional chlorophyll fluorometers. *New*
744 *Phytologist*, **191**, 146-159.
745 Oya V.M. & Laisk A.K. (1976) Adaptation of the photosynthesis apparatus to the light profile in
746 the leaf. *Soviet Plant Physiology*, **23**, 381–386.
747 Parkhurst D.F. (1986) Internal leaf structure: a three-dimensional perspective. In: *On the*
748 *economy of plant form and function* (ed T. Givnish), pp. 215-249. Cambridge University
749 Press.
750 Parkhurst D.F. (1994) Diffusion of CO_2 and other gases inside leaves. *New Phytologist*, **126**,
751 449-479.
752 Perez-Martin A., Michelazzo C., Torres-Ruiz J.M., Flexas J., Fernández J.E., Sebastiani L. &
753 Diaz-Espejo A. (2014) Regulation of photosynthesis and stomatal and mesophyll
754 conductance under water stress and recovery in olive trees: correlation with gene
755 expression of carbonic anhydrase and aquaporins. *Journal of Experimental Botany*, **65**,
756 3143-3156.
757 Piel C., Frak E., Le Roux X. & Genty B. (2002) Effect of local irradiance on CO_2 transfer
758 conductance of mesophyll in walnut. *Journal of Experimental Botany*, **53**, 2423-2430.
759 Prado K., Boursiac Y., Tournaire-Roux C., Monneuse J-M., Postaire O., Da Ines O., Schäffner
760 A.R., Hem S., Santoni V. & Maurel C. (2013) Regulation of *Arabidopsis* leaf hydraulics
761 involves light-dependent phosphorylation of aquaporins in veins. *The Plant Cell*, **25**,
762 1029-1039.

763 Russin W.A. & Trivett C.L. (2001) Vacuum-microwave combination for processing plant tissues
764 for electron microscopy. *Microwave Techniques and Protocols*, 25-35.
765 Schneider, C.A., Rasband, W.S. & Eliceiri, K.W. (2012) NIH Image to ImageJ: 25 years of
766 image analysis. *Nature Methods*, **9**, 671-675.
767 Schäeufele R., Santrucek J. & Schnyder H. (2011) Dynamic changes of canopy-scale mesophyll
768 conductance to CO_2 diffusion of sunflower as affected by CO_2 concentration and abscisic
769 acid. *Plant, Cell & Environment*, **34**, 127-136.
770 Tazoe Y., von Caemmerer S., Badger M.R. & Evans J.R. (2009) Light and CO_2 do not affect the
771 mesophyll conductance to CO_2 diffusion in wheat leaves. *Journal of Experimental*
772 *Botany*, **60**, 2291-2301.
773 Terashima, I. (1986) Dorsiventrality in photosynthetic light response curves of a leaf. *Journal of*
774 *Experimental Botany*, **37**, 399-405.
775 Terashima, I., Fujita, T. Inoue, T., Soon Chow, W. & Oguchi, R. (2009) Green light drives leaf
776 photosynthesis more efficiently than red light in strong white light: revisiting the
777 enigmatic question of why leaves are green. *Plant and Cell Physiology*, **50**, 684-697.
778 Terashima I., Hanba Y.T., Tholen D. & Niinemets Ü. (2011) Leaf functional anatomy in relation
779 to photosynthesis. *Plant Physiology*, **155**, 108-116.
780 Terashima I. & Inoue Y. (1985) Vertical gradient in photosynthetic properties of spinach
781 chloroplast dependent on intra-leaf light environment. *Plant and Cell Physiology*, **26**,
782 781-785.
783 Terashima I., Sakaguchi S. & Hara N. (1986) Intra-leaf and intracellular gradients in chloroplast
784 ultrastructure of dorsiventral leaves illuminated from the adaxial or abaxial side during
785 their development. *Plant and Cell Physiology*, **27**, 1023-1031.

786 Thain J. (1983) Curvature correction factors in the measurement of cell surface areas in plant
787 tissues. *Journal of Experimental Botany*, **34**, 87-94.
788 Théroux-Rancourt G., Éthier G. & Pepin S. (2014) Threshold response of mesophyll CO_2
789 conductance to leaf hydraulics in highly transpiring hybrid poplar clones exposed to soil
790 drying. *Journal of Experimental Botany*, **65**, 741-753.
791 Tholen D., Boom C., Noguchi K.O., Ueda S., Katase T. & Terashima I. (2008) The chloroplast
792 avoidance response decreases internal conductance to CO2 diffusion in *Arabidopsis*
793 *thaliana* leaves. *Plant, Cell & Environment*, **31**, 1688–1700.
794 Tholen D. & Zhu X.-G. (2011) The mechanistic basis of internal conductance: a theoretical
795 analysis of mesophyll cell photosynthesis and CO_2 diffusion. *Plant Physiology*, **156**, 90-
796 105.
797 Verboven P., Herremans E., Helfen L., Ho Q.T., Abera M., Baumbach T., Wevers M. & Nicolaï
798 B.M. (2015) Synchrotron X-ray computed laminography of the three-dimensional
799 anatomy of tomato leaves. *The Plant Journal*, **81**, 169-182.
800 Vogelmann, T.C. (1993) Plant tissue optics. *Annual Review of Plant Physiology and Plant*
801 *Molecular Biology*, **44**, 231–251.
802 Vogelmann T. & Han T. (2000) Measurement of gradients of absorbed light in spinach leaves
803 from chlorophyll fluorescence profiles. *Plant, Cell & Environment*, **23**, 1303-1311.
804 Vrábl D., Vašková M., Hronková M., Flexas J. & Šantrůček J. (2009) Mesophyll conductance to
805 CO_2 transport estimated by two independent methods: effect of variable CO_2
806 concentration and abscisic acid. *Journal of Experimental Botany*, **60**, 2315–2323.

807 Yamori W., Evans J.R. & Von Caemmerer S. (2010) Effects of growth and measurement light
808 intensities on temperature dependence of CO_2 assimilation rate in tobacco leaves. *Plant,*
809 *Cell & Environment*, **33**, 332-343.
810 Yin X., Struik P.C., Romero P., Harbinson J., Evers J.B., Van Der Putten P.E. & Vos J. (2009)
811 Using combined measurements of gas exchange and chlorophyll fluorescence to estimate
812 parameters of a biochemical C3 photosynthesis model: a critical appraisal and a new
813 integrated approach applied to leaves in a wheat (*Triticum aestivum*) canopy. *Plant, Cell*
814 *& Environment*, **32**, 448-464.

APPENDIX

Summary of Lloyd *et al.*'s (1992) derivation of g_m accounting for structural variations in photosynthetic characteristics across a leaf

Lloyd *et al*. (1992) presented a mathematically sophisticated approach to calculate $g_{m,leaf}$ to account for variations in photosynthetic characteristics across a leaf, building on what Terashima and Inoue (1985) presented before. Briefly, they considered volume-based variables so that (eqn. A1.1 in the original paper):

$$A_{n,leaf} = \int_0^t A_v dx \qquad \text{(eqn. 17)}$$

where *t* is the thickness of the leaf and *x* is the distance above the abaxial surface. Keeping this volume-based approach and using carbon isotopic discrimination equations (eqn. A1.2-1.4 in the original paper), they derived an estimated leaf conductance to CO_2 as (their eqn. A1.5):

$$g_{m,leaf} = \frac{\left(\int_0^t A_v dx\right)^2}{\int_0^t \left(\frac{A_v^2}{g_v}\right) dx} \qquad \text{(eqn. 18)}$$

which can be converted to a leaf area based expression, as the sum of each layer *j* for a leaf consisting of *l* layers:

$$g_{m,leaf} = \frac{\left(\sum_{j=1}^{l} A_{n,j}\right)^2}{\sum_{j=1}^{l} {A_{n,j}}^2 / g_{m,j}} \qquad \text{(eqn. 19)}$$

This equation of Lloyd *et al*. (1992) can be simplified to result in eqn. 9. Rearranging eqn. 19 and substituting eqn. 5 for $g_{m,j}$:

$$g_{m,leaf} = \frac{\left(\sum_{j=1}^{l} A_{n,j}\right)^2}{\sum_{j=1}^{l} A_{n,j}(C_{i,j}-C_{c,j})} \quad \text{(eqn. 20)}$$

If $C_{i,j}$ is assumed to be the same for all layers (i.e. C_i), then the equation can be rearranged:

$$g_{m,leaf} = \frac{\left(\sum_{j=1}^{l} A_{n,j}\right)^2}{C_i \sum_{j=1}^{l} A_{n,j} - \sum_{j=1}^{l} A_{n,j} C_{c,j}} \quad \text{(eqn. 21)}$$

and dividing the numerator and denominator by $\sum_{j=1}^{l} A_{n,j}$, then:

$$g_{m,leaf} = \frac{\sum_{j=1}^{l} A_{n,j}}{\frac{C_i \sum_{j=1}^{l} A_{n,j}}{\sum_{j=1}^{l} A_{n,j}} - \frac{\sum_{j=1}^{l} A_{n,j} C_{c,j}}{\sum_{j=1}^{l} A_{n,j}}} \quad \text{(eqn. 22)}$$

By simplification, and replacing the numerator with $A_{n,leaf}$ ($=\sum_{j=1}^{l} A_{n,j}$) we get eqn. 9.

Alternative derivation for leaf g_m based upon different photosynthetic layers

A simpler derivation of eqn. 9 starts with defining leaf apparent g_m as:

$$g_{m,leaf} = \frac{A_{n,leaf}}{C_i - C_{c,wt}} \quad \text{(eqn. 23)}$$

assuming that C_i is the same for all leaf layers. $C_{c,wt}$ is then the apparent value, the weighted average for the many cell layers. If weighted by layer photosynthesis, similar to eqn. A1.20 (Lloyd *et al.* 1992):

$$C_{c,wt} = \frac{\sum_{j=1}^{l} A_{n,j} C_{c,j}}{\sum_{j=1}^{l} A_{n,j}} \quad \text{(eqn. 24)}$$

As $A_{n,leaf}$ is a sum of layer $A_{n,j}$:

$$A_{n,leaf} = \sum_{j=1}^{l} A_{n,j} \quad \text{(eqn. 25)}$$

Then substituting eqn. 25 into eqn. 23 we get eqn. 9:

$$g_{m,leaf} = \frac{A_{n,leaf}}{C_i - \frac{\sum_{j=1}^{l} A_{n,j} C_{c,j}}{A_{n,leaf}}} \quad \text{(eqn. 9)}$$

This equation has the expected property that when a particular $A_{n,j}$ tends towards zero, then that layer's $C_{c,j}$ is a decreasing component of the calculation of leaf weighted C_c.

855 **Table 1.** Mathematical terms used in the model

Name	Symbol	Value and units
Absorptance of layer *j*	α_j	[-]
Partitioning factor of α_j to PSII	β_j	0.5 [-]
Compensation point of layer *j*	Γ^*_j	37.4[a] μmol mol^{-1}
Light response curvature factor for layer *j*	θ_j	[-]
Net photosynthesis of leaf and layer *j*	$A_{n,leaf}$, $A_{n,j}$	μmol m^{-2} s^{-1}
Net photosynthesis on volume basis	A_v	μmol μm^{-3} s^{-1}
Chloroplastic [CO_2] of leaf and layer *j*	C_c,$C_{c,j}$	μmol mol^{-1}
C_c value for leaf weighted by layer	$C_{c,wt}$	μmol mol^{-1}
Intercellular CO_2 concentration of leaf	C_i	μmol mol^{-1}
A correction for spectral quality of light	f_j	0.15 [-]
Mesophyll conductance of leaf or cell layer *j*	$g_{m,leaf}$, $g_{m,j}$	mol m^{-2} s^{-1}
Irradiance used by PSII of layer *j*	$I_{2,j}$	μmol m^{-2} s^{-1}
Index representing layers of cells	*j*	
Electron transport rate of layer *j*	J_j	μmol m^{-2} s^{-1}
Maximum electron transport rate of layer *j*	$J_{max,j}$	μmol m^{-2} s^{-1}
Michaelis constant for Rubisco carboxylation	$K_{c,j}$	272.4[a] μmol mol^{-1}
Michaelis constant for Rubisco oxygenation	$K_{o,j}$	165.8[a] mol mol^{-1}
Total layers of cells modelled in leaf	*l*	2 to 3
Oxygen concentration	O	200 mmol mol^{-1}
Photosynthetic photon flux density	PPFD	μmol m^{-2} s^{-1}

PPFD incident on layer *j*	$PPFD_j$	μmol m^{-2} s^{-1}
Day respiration of layer *j*	$R_{d,j}$	μmol m^{-2} s^{-1}
Rate of Rubisco carboxylation of layer *j*	$V_{c,Rubisco,j}$	μmol m^{-2} s^{-1}
Rate of RuBP-regeneration of layer *j*	$V_{c,RuBP,j}$	μmol m^{-2} s^{-1}

856 [a] photosynthetic parameters taken from Bernacchi *et al*. (2002)

857

858 **Table 2.** Anatomical measurements of three evenly spaced layers in leaf profiles of *Arbutus* and

859 *Triticum*.

Species	*Arbutus*				*Triticum*			
Layer	Whole	Adaxial	Middle	Abaxial	Whole	Adaxial	Middle	Abaxial
Mesophyll thickness (µm)	236 (8)[a]				148 (18)			
Porosity (%)	25 (2)	11 (1)	26 (2)	37 (6)	24 (1)	20 (3)	20 (3)	31 (4)
S_m (µm^2 µm^{-2})	25.9 (2.4)	9.2 (1.0)	8.9 (0.8)	7.0 (0.6)	20.2 (1.6)	6.3 (0.5)	5.7 (1.0)	7.0 (0.7)
S_c (µm^2 µm^{-2})	21.8 (1.7)	8.2 (0.9)	8.3 (0.7)	5.2 (0.4)	17.6 (1.0)	6.0 (0.5)	4.9 (0.9)	6.7 (0.7)
S_c / whole leaf S_c		0.38	0.38	0.24		0.34	0.27	0.39
F[b]		1.50	1.42	1.23		1.45	1.40	1.45
Nb. of cell layers	7	1	2	4	4	1	2	1
T_{cw} (µm)		0.35 (0.04)	0.38 (0.12)	0.37 (0.05)		0.13 (0.04)	0.18 (0.03)	0.13 (0.04)
T_{cyt} (µm)		0.39 (0.03)	0.25 (0.11)	0.36 (0.05)		0.10 (0.01)	0.11 (0.02)	0.10 (0.01)
g'_{liq} (mmol m^{-2} chloroplast s^{-1})[c]	52 (5)	20 (1)	19 (3)	15 (1)	81(4)	28 (2)	26 (1)	28 (2)
g_m (g'_{liq} × S_c; mol m^{-2} s^{-1})[c]	0.39 (0.04)	0.16 (0.01)	0.15 (0.02)	0.08 (0.01)	0.48 (0.03)	0.17 (0.01)	0.13 (0.01)	0.19 (0.01)

860 [a] Standard deviation in parenthesis. Five cross-sections measured for each species (two different

861 leaves per species).

862 [b] Curvature correction factor, based on the method of Thain (1983). The value for *Triticum* is in

863 agreement with values for other grasses e.g. 1.42 for *Oryza* sp. (Giuliani *et al.* 2013).

864 [c] Estimated anatomical features made using methods in Evans *et al*. (2009).

865

FIGURE LEGENDS

Figure 1. Simulated bulk leaf mesophyll conductance ($g_{m,leaf}$) response to PPFD based upon modelling photosynthesis of multiple layers (j) of cells with differential penetration of PPFD with depth (top right). The estimation of $g_{m,leaf}$ is undefined when $A_{n,leaf}$ is close to zero (see eqn. 9), and such values were removed from the top right curve. Detailed simulation values across a three-layer leaf cross section for 65, 100, and 1500 µmol m^{-2} s^{-1} PPFD are shown on the bottom row, with the gradient in light within the leaf represented by the shade gradient from adaxial to abaxial epidermis (general mesophyll cell model of photosynthesis for the path from C_i to $A_{n,j}$ shown on top left). The simulation was run for the null model of a three layer leaf, each with identical photosynthetic parameters, including: α_j = 0.6, $g_{m,j}$ = 0.1 mol m^{-2} s^{-1}, $J_{max,j}$ = 200 µmol m^{-2} s^{-1}, θ_j = 0.6, and $R_{d,j}$ = 1 µmol m^{-2} s^{-1} per layer. The un-italicized value for $g_{m,j}$ was the constant for each layer as set in the model, the italicized value was the weighted value used to calculate total leaf $g_{m,leaf}$ using eqn. 9. Units in the figure: C_c and C_i, µmol mol^{-1}; g_m, mol m^{-2} s^{-1}; A_n, µmol m^{-2} s^{-1}.

Figure 2. Measured responses of leaf total net photosynthesis ($A_{n,leaf}$) and leaf total mesophyll conductance ($g_{m,leaf}$) to PPFD for the two species, with adaxial (black points) or abaxial illumination (gray points). Shaded regions represent the range of fitted values, with the median shown as a solid line, from all the solutions within 10% of the SSE of the best solution, using a three layer model of leaf photosynthesis (fitted values of α_j, $g_{m,j}$, $J_{max,j}$, θ_j and $R_{d,j}$ are shown in Fig. 6). Error bars represent standard errors of the mean for five plants.

888 **Figure 3.** Independent validation of the variable J method of measuring bulk leaf mesophyll
889 conductance (g_m variable J) by comparison to simultaneous measurement of g_m using the stable
890 isotope method (g_m SI). Light response curves of g_m for adaxial (black) and abaxial (gray)
891 illumination of leaves are shown for one representative leaf of *Arbutus* (circles) and *Triticum*
892 (squares).

893

894 **Figure 4.** Micrographs of leaf anatomy of *Arbutus* and *Triticum*. Cross sections (top row) are
895 shown at the same scale (width of each image: 341 μm). Dotted lines show where the layers
896 were cut for the parameters measured and presented in Table 2. TEM micrographs (bottom row)
897 present cells from the adaxial (Ad), middle (Mid), and abaxial (Ab) layers for each species (left
898 to right), showing differences in cell wall thickness. Vacuoles in *Arbutus* that are dark grey
899 contain polyphenols as these stain with methylene blue.

900

901 **Figure 5.** The modelled response of net photosynthesis per leaf layer ($A_{n,j}$) for a three layer leaf
902 for adaxial and abaxial illumination for the adaxial (Ad; red), middle (Mid; green), and abaxial
903 (Ab; blue) mesophyll layers. All predicted layer specific light response curves from the solutions
904 within 10% of the SSE of the best solution are presented, and the thick tinted lines represent the
905 median value. Mesophyll conductance values per layer were modelled as constant, but total leaf
906 values varied according to eqn. 9. The modelled curves in these panels result in the fit to the data
907 shown in Fig. 2. Adaxial and middle layers values for *Arbutus* under adaxial illumination are
908 mostly similar and the lines are superimposed.

909

Figure 6. Distribution of the layer-specific parameters from the optimization solutions that were within 10% of the SSE of the best solution from 500 optimizations using different starting sets of values. Black dots represent the median of layer-specific values, and gray lines show the predicted relative profile based on S_c (for $J_{max,j}$ and $R_{d,j}$) and g_m estimated from leaf anatomy (Table 2). Number of solutions within 10% of the best solution: *Arbutus*, n = 340; *Triticum*, n = 33.

Figure 7. Predicted profiles of the fraction of light absorbed for adaxial and abaxial illumination for *Arbutus* and *Triticum*. Predicted data (black points) are compared to values for a bifacial (spinach for *Arbutus*; Evans and Vogelmann 2003) and isobilateral leaf (eucalyptus for *Triticum*; Evans and Vogelmann 2006). Both these studies generated profiles from the relative ^{14}C assimilation profiles for blue (solid line) and green light (dashed line). Predicted profiles were computed from the median layer-specific light absorptance value (Fig. 6), and profiles from literature values were computed by dividing the leaf into three layers and summing up the relative absorptance over each layer for both ad- and abaxial profiles.

Figure 8. Proportional sensitivity analysis of simulated $g_{m,leaf}$ response to PPFD. The values for five parameters in the lower layer of a two layer leaf were decreased by 50%, and the values shown are the percent change in $g_{m,leaf}$ following that decrease. PPFD values are shown on a log scale to highlight changes under low and high light intensities. The default model of $g_{m,leaf}$ response to PPFD had both layers of the leaf with the same photosynthetic parameters ($g_{m,j}$ = 0.1 µmol m^{-2} s^{-1}, $R_{d,j}$ = 1 µmol m^{-2} s^{-1}, α_j = 0.75, θ_j = 0.8, $J_{max,j}$ = 50 µmol m^{-2} s^{-1}). The estimation

of $g_{m,leaf}$ when $A_{n,leaf}$ is close to zero is undefined because of how the assimilated weighted $g_{m,leaf}$ is computed (eqn. 9), and such values were removed from the sensitivity analysis.

Figure 9. General responses of net photosynthesis ($A_{n,leaf}$) and $g_{m,leaf}$ to PPFD modelled with the null model (same as Fig. 1; all parameters equal for all layers), a leaf with low $J_{max,j}$ (same as null model, but with $J_{max,j}$ = 10 µmol m^{-2} s^{-1} and $R_{d,j}$ = 0.05 µmol m^{-2} s^{-1}), a leaf with a decreasing gradient of $g_{m,j}$ with depth (same as null model but with $g_{m,j}$ of 0.15, 0.10, and 0.05 mol m^{-2} s^{-1} for the adaxial, middle, and abaxial layers), or increasing absorptance (α_j) with depth (same as null model, but with α_j of 0.25, 0.50, and 0.75 for the adaxial, middle, and abaxial layers). The estimation of $g_{m,leaf}$ when $A_{n,leaf}$ is close to zero is undefined because of how the assimilated weighted $g_{m,leaf}$ is computed (eqn. 9), and such values were removed from the fitted responses. Other photosynthetic parameters were kept constant (α_j = 0.6, $g_{m,j}$ = 0.1 mol m^{-2} s^{-1}, $J_{max,j}$ = 200 µmol m^{-2} s^{-1}, θ_j = 0.6, and $R_{d,j}$ = 1 µmol m^{-2} s^{-1} per layer).

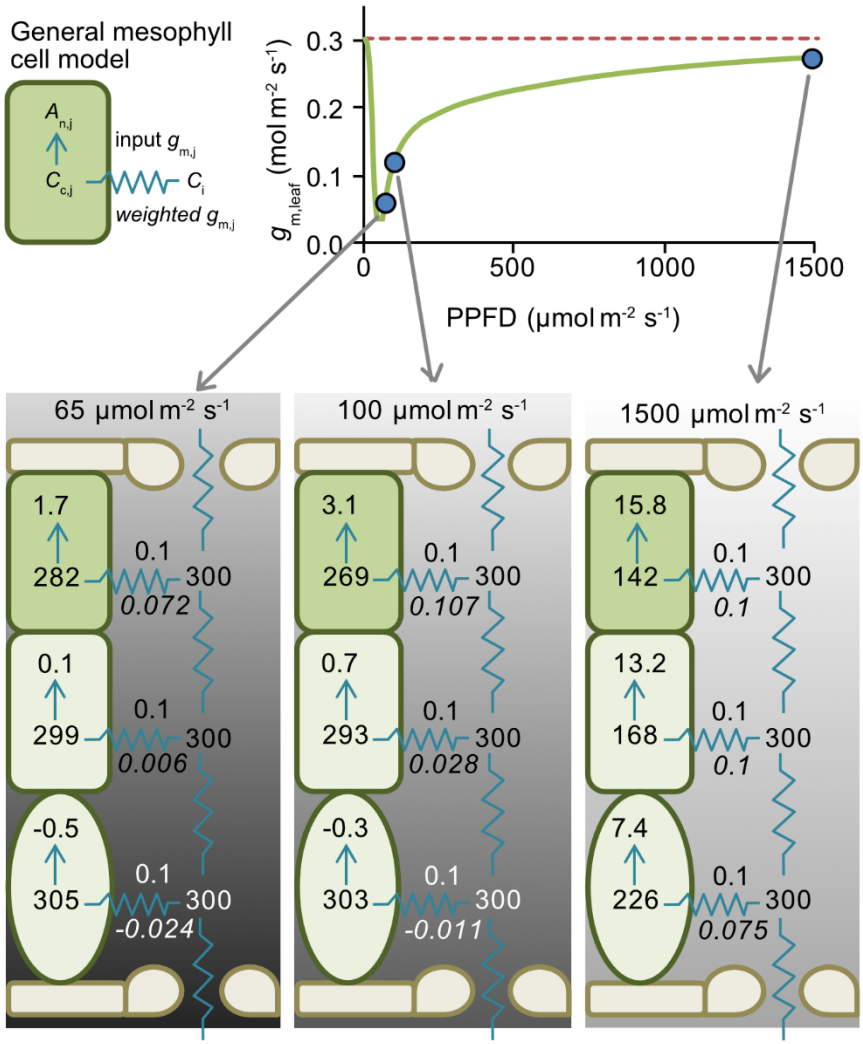

945

946 **Figure 1.** Simulated bulk leaf mesophyll conductance ($g_{m,leaf}$) response to PPFD based upon
947 modelling photosynthesis of multiple layers (j) of cells with differential penetration of PPFD
948 with depth (top right). The estimation of $g_{m,leaf}$ is undefined when $A_{n,leaf}$ is close to zero (see eqn.
949 9), and such values were removed from the top right curve. Detailed simulation values across a
950 three-layer leaf cross section for 65, 100, and 1500 µmol m^{-2} s^{-1} PPFD are shown on the bottom
951 row, with the gradient in light within the leaf represented by the shade gradient from adaxial to
952 abaxial epidermis (general mesophyll cell model of photosynthesis for the path from C_i to $A_{n,j}$
953 shown on top left). The simulation was run for the null model of a three layer leaf, each with

identical photosynthetic parameters, including: α_j = 0.6, $g_{m,j}$ = 0.1 mol m^{-2} s^{-1}, $J_{max,j}$ = 200 µmol m^{-2} s^{-1}, θ_j = 0.6, and $R_{d,j}$ = 1 µmol m^{-2} s^{-1} per layer. The un-italicized value for $g_{m,j}$ was the constant for each layer as set in the model, the italicized value was the weighted value used to calculate total leaf $g_{m,leaf}$ using eqn. 9. Units in the figure: C_c and C_i, µmol mol^{-1}; g_m, mol m^{-2} s^{-1}; A_n, µmol m^{-2} s^{-1}.

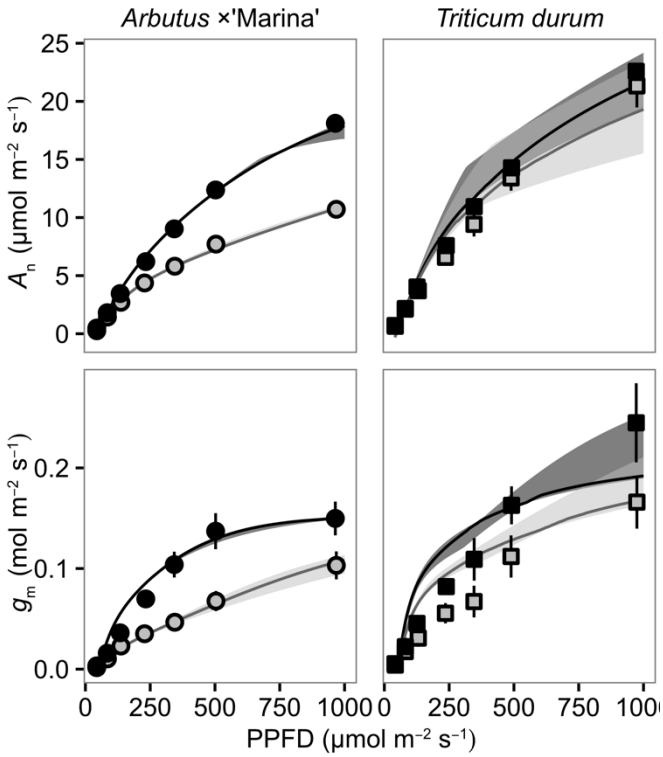

959

960 **Figure 2.** Measured responses of leaf total net photosynthesis ($A_{n,leaf}$) and leaf total mesophyll
961 conductance ($g_{m,leaf}$) to PPFD for the two species, with adaxial (black points) or abaxial
962 illumination (gray points). Shaded regions represent the range of fitted values, with the median
963 shown as a solid line, from all the solutions within 10% of the SSE of the best solution, using a
964 three layer model of leaf photosynthesis (fitted values of α_j, $g_{m,j}$, $J_{max,j}$, θ_j and $R_{d,j}$ are shown in
965 Fig. 6). Error bars represent standard errors of the mean for five plants.

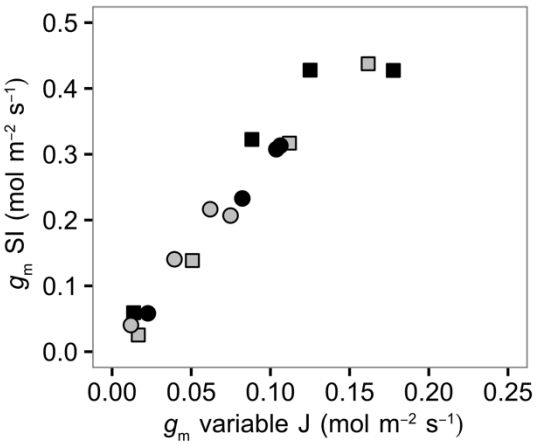

966

967 **Figure 3.** Independent validation of the variable J method of measuring bulk leaf mesophyll
968 conductance (g_m variable J) by comparison to simultaneous measurement of g_m using the stable
969 isotope method (g_m SI). Light response curves of g_m for adaxial (black) and abaxial (gray)
970 illumination of leaves are shown for one representative leaf of *Arbutus* (circles) and *Triticum*
971 (squares).

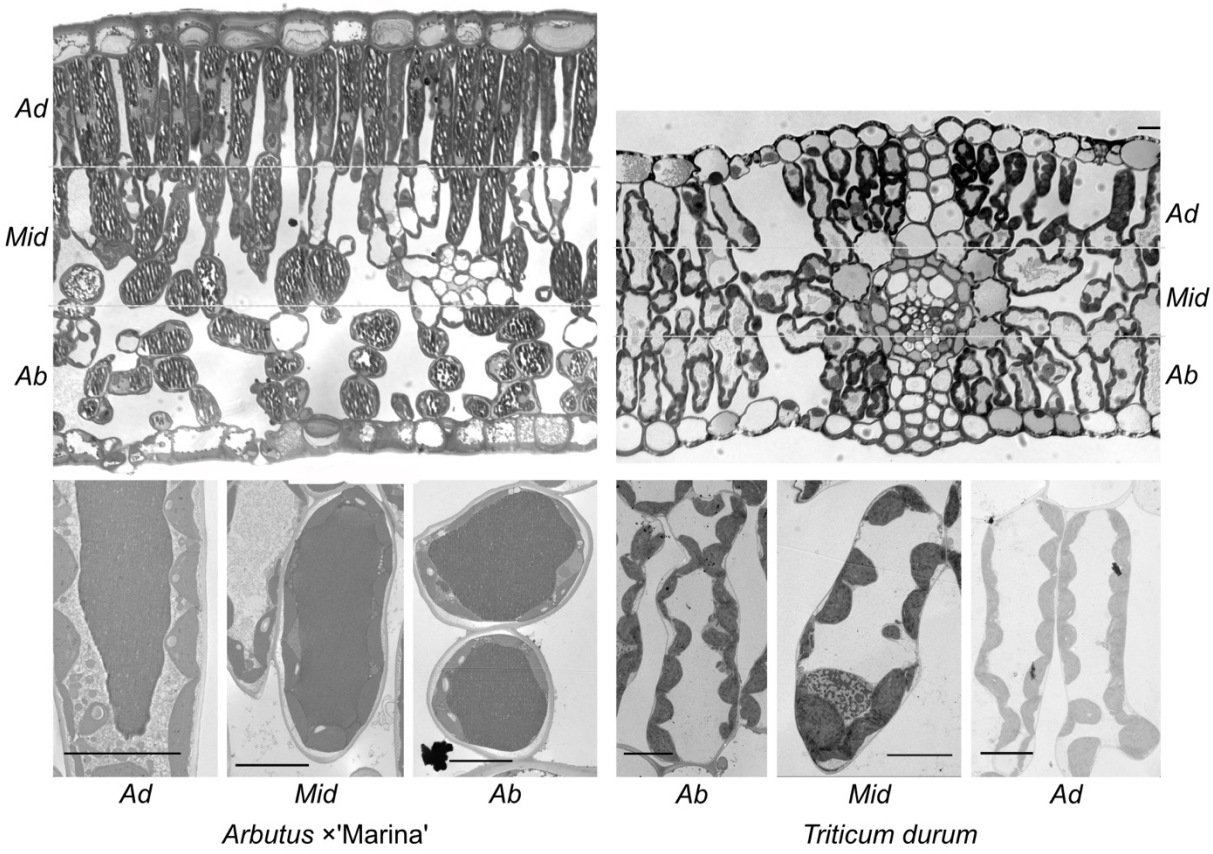

Figure 4. Micrographs of leaf anatomy of *Arbutus* and *Triticum*. Cross sections (top row) are shown at the same scale (width of each image: 341 µm). Dotted lines show where the layers were cut for the parameters measured and presented in Table 2. TEM micrographs (bottom row) present cells from the adaxial (Ad), middle (Mid), and abaxial (Ab) layers for each species (left to right), showing differences in cell wall thickness. Vacuoles in *Arbutus* that are dark grey contain polyphenols as these stain with methylene blue.

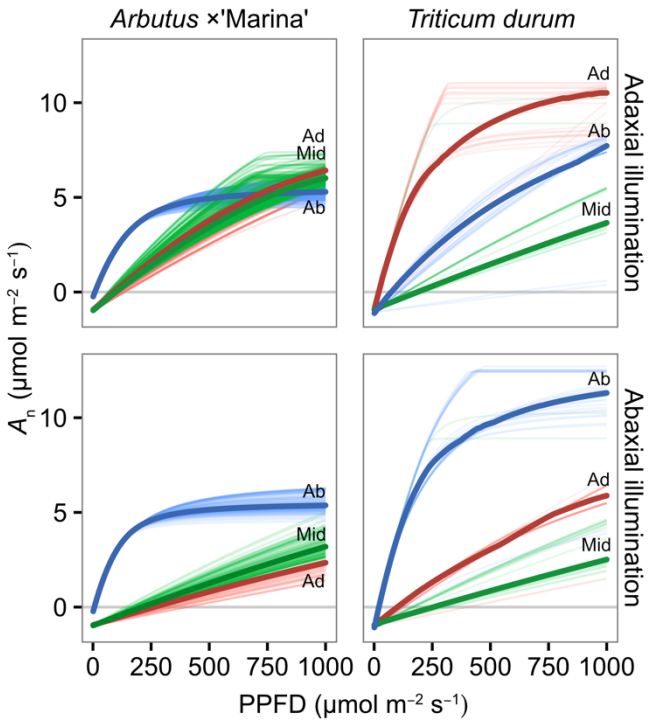

Figure 5. The modelled response of net photosynthesis per leaf layer ($A_{n,j}$) for a three layer leaf for adaxial and abaxial illumination for the adaxial (Ad; red), middle (Mid; green), and abaxial (Ab; blue) mesophyll layers. All predicted layer specific light response curves from the solutions within 10% of the SSE of the best solution are presented, and the thick tinted lines represent the median value. Mesophyll conductance values per layer were modelled as constant, but total leaf values varied according to eqn. 9. The modelled curves in these panels result in the fit to the data shown in Fig. 2. Adaxial and middle layers values for *Arbutus* under adaxial illumination are mostly similar and the lines are superimposed.

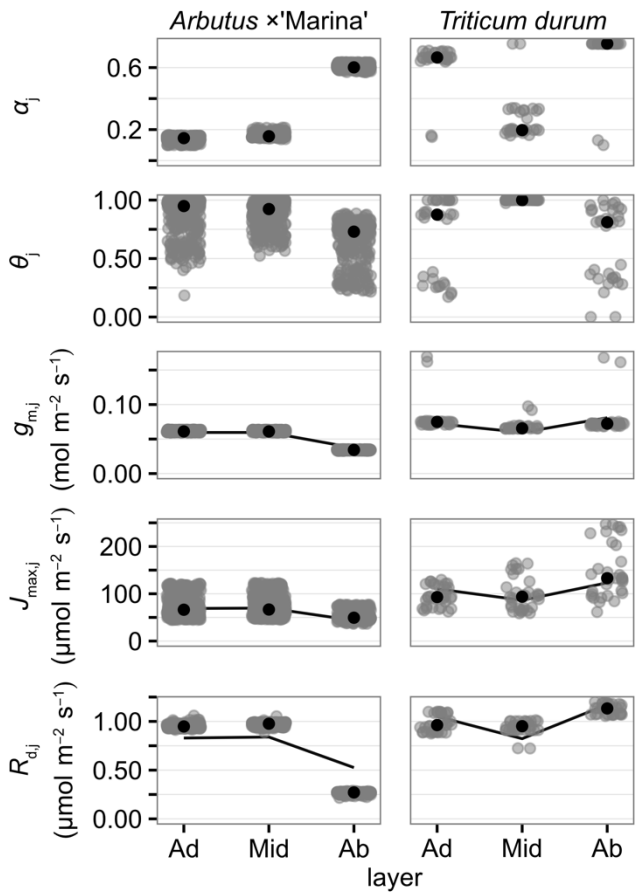

988

989 **Figure 6.** Distribution of the layer-specific parameters from the optimization solutions that were
990 within 10% of the SSE of the best solution from 500 optimizations using different starting sets of
991 values. Black dots represent the median of layer-specific values, and gray lines show the
992 predicted relative profile based on S_c (for $J_{max,j}$ and $R_{d,j}$) and g_m estimated from leaf anatomy
993 (Table 2). Number of solutions within 10% of the best solution: *Arbutus*, n = 340; *Triticum*, n =
994 33.

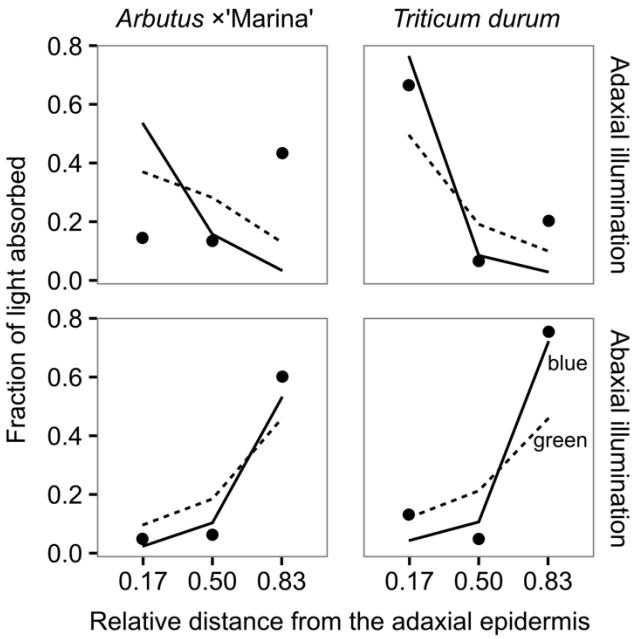

Figure 7. Predicted profiles of the fraction of light absorbed for adaxial and abaxial illumination for *Arbutus* and *Triticum*. Predicted data (black points) are compared to values for a bifacial (spinach for *Arbutus*; Evans and Vogelmann 2003) and isobilateral leaf (eucalyptus for *Triticum*; Evans and Vogelmann 2006). Both these studies generated profiles from the relative ^{14}C assimilation profiles for blue (solid line) and green light (dashed line). Predicted profiles were computed from the median layer-specific light absorptance value (Fig. 6), and profiles from literature values were computed by dividing the leaf into three layers and summing up the relative absorptance over each layer for both ad- and abaxial profiles.

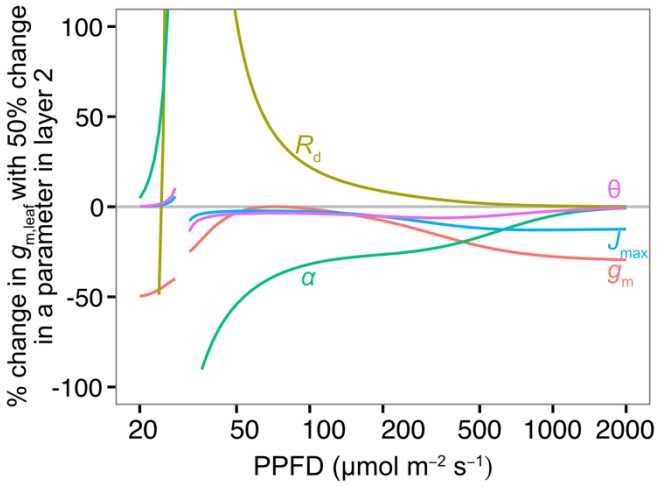

Figure 8. Proportional sensitivity analysis of simulated $g_{m,leaf}$ response to PPFD. The values for five parameters in the lower layer of a two layer leaf were decreased by 50%, and the values shown are the percent change in $g_{m,leaf}$ following that decrease. PPFD values are shown on a log scale to highlight changes under low and high light intensities. The default model of $g_{m,leaf}$ response to PPFD had both layers of the leaf with the same photosynthetic parameters ($g_{m,j}$ = 0.1 µmol m^{-2} s^{-1}, $R_{d,j}$ = 1 µmol m^{-2} s^{-1}, α_j = 0.75, θ_j = 0.8, $J_{max,j}$ = 50 µmol m^{-2} s^{-1}). The estimation of $g_{m,leaf}$ when $A_{n,leaf}$ is close to zero is undefined because of how the assimilated weighted $g_{m,leaf}$ is computed (eqn. 9), and such values were removed from the sensitivity analysis.

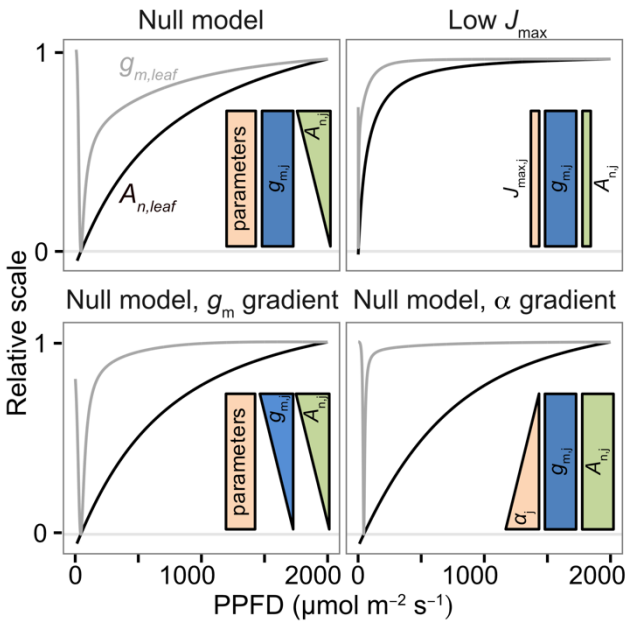

Figure 9. General responses of net photosynthesis ($A_{n,leaf}$) and $g_{m,leaf}$ to PPFD modelled with the null model (same as Fig. 1; all parameters equal for all layers), a leaf with low $J_{max,j}$ (same as null model, but with $J_{max,j}$ = 10 µmol m^{-2} s^{-1} and $R_{d,j}$ = 0.05 µmol m^{-2} s^{-1}), a leaf with a decreasing gradient of $g_{m,j}$ with depth (same as null model but with $g_{m,j}$ of 0.15, 0.10, and 0.05 mol m^{-2} s^{-1} for the adaxial, middle, and abaxial layers), or increasing absorptance (α_j) with depth (same as null model, but with α_j of 0.25, 0.50, and 0.75 for the adaxial, middle, and abaxial layers). The estimation of $g_{m,leaf}$ when $A_{n,leaf}$ is close to zero is undefined because of how the assimilated weighted $g_{m,leaf}$ is computed (eqn. 9), and such values were removed from the fitted responses. Other photosynthetic parameters were kept constant (α_j = 0.6, $g_{m,j}$ = 0.1 mol m^{-2} s^{-1}, $J_{max,j}$ = 200 µmol m^{-2} s^{-1}, θ_j = 0.6, and $R_{d,j}$ = 1 µmol m^{-2} s^{-1} per layer).